Long Non-Coding RNA TMEM220-AS1 Suppressed Hepatocellular Carcinoma by Regulating the miR-484/MAGI1 Axis as a Competing Endogenous RNA

Cong Cao
The Affiliated Hospital of Youjiang Medical University for Nationalities
Jun Li
The Affiliated Hospital of Youjiang Medical University for Nationalities
Guangzhi Li
The Affiliated Hospital of Youjiang Medical University for Nationalities
Gaoyu Hu
The Affiliated Hospital of Youjiang Medical University for Nationalities
Zhihua Deng
The Affiliated Hospital of Youjiang Medical University for Nationalities
Bing Huang
The Affiliated Hospital of Youjiang Medical University for Nationlities
Jing Yang
The Affiliated Hospital of Youjiang Medical University for Nationalities
Jiequn Li
The Second Affiliated Hospital of Guangxi Medical University
Song Cao (13877189102@163.com)
Zhongnan University Affiliated Xiangya Second Hospital

Research

Keywords: hepatocellular carcinoma, Long non-coding RNA, TMEM220-AS1, cell invasion, EMT

Posted Date: October 9th, 2020

DOI: https://doi.org/10.21203/rs.3.rs-88668/v1

Version of Record: A version of this preprint was published at Frontiers in Cell and Developmental Biology on August 5th, 2021. See the published version at https://doi.org/10.3389/fcell.2021.681529.

Abstract

Background

Long non-coding RNA has a considerable regulative influence in multiple biological processes. Nevertheless, the role of TMEM220-AS1 in hepatocellular carcinoma (HCC) remains unclear.

Methods

We used the TCGA database to analyze differentially expressed lncRNAs. qRT-PCR was used to verify the results in a large population. Afterwards, *in vitro* effects of TMEM220-AS1 on HCC cells were determined by CCK-8, EdU, Flow cytometry experiment and transwell assays in HCC cells. We adopted qRT-PCR, western blot to identify epithelial-mesenchymal transition (EMT). Moreover, we adopted bioinformatics analysis, western blot, dual luciferase reporter gene assay and RIP to investigate underlying molecular mechanisms of TMEM220-AS1 function. Finally, the function of TMEM220-AS1 was verified *in vivo*.

Results

TMEM220-AS1 was remarkably decreasedin HCC. It was demonstrated that malignant phenotypes and EMT of HCC cells were promoted by knocking TMEM220-AS1 down both *in vivo* and *in vitro*. TMEM220-AS1, which was detected distributing mainly in the cytoplasm, worked as a miRNA sponge to sponge miR-484 and promote the level of MAGI1, therefore curbed malignant phenotypes of HCC cells.

Conclusions

In conclusion, downregulation of TMEM220-AS1promotes HCC through miR-484/MAGI1 axis.

Background

As the sixth most frequent cancer worldwide, liver cancer is the third prior cause of cancer-related deaths[1-3]. Inall of the primary liver cancers, hepatocellular carcinoma (HCC) is the most frequent, responsible for 80%–90% of all cases[4]. Hepatocellular carcinoma, which is one of the most aggressive and resistant cancers, has a bad prognosis[5]. In the United States and many other countries, the morbidity of HCC has doubled over the past two decades. Annually, the number of those diagnosed with HCC adds up to almost 800,000 worldwide, with approximately 750,000 causalities[6, 7]. Concerning the development of HCC, chronic hepatitis B and C virus infection were placed the most common risk factors and responsible for approximately 75% of HCCs, likely leading to HCC development increase twenty-fold[7]. There are other major risk factors, including nonalcoholic fatty liver disease (NAFLD), aflatoxin B1 (AFB1) exposure obesity and chronic alcohol consumption[8]. However, the molecular mechanism implicated in the pathogenesis of HCC is still under intense investigation.

Recently, increasing evidence identified lncRNAs as vital regulators in numerous cancers, with HCC included[9, 10]. Through numerous mechanisms, lncRNA abnormal expression exerts considerable

influence on cancer progression and carcinogenesis[11, 12]. To give an instance,LINC00346 modulates CDK1/CCNB1 axis, consequently regulating the development of hepatocellular carcinoma, serving as a competing endogenous RNA[13]. In hepatocellular carcinoma, LINC00160 is able to mediate drug resistance and autophagy, which is through microRNA-132/PIK3R3 axis[14].Modifying genomic methylation profiles, LINC00662 can promote progression of hepatocellular carcinoma progression[15].

We used the TCGA database to analyze the differentially expressed lncRNAs and found that TMEM220-AS1 was poorly expressed in HCC. However, we didn't know whether TMEM220-AS1 was correlated to the development of HCC. Here, we determined to uncover the function of TMEM220-AS1in HCC. To address this issue, we performed a large sample validation in a population, followed by a series of cell function tests, dual luciferase reporter gene assay, bioinformatics analysis, western blot assay, and RIP to explore underlying molecular mechanisms of TMEM220-AS1 function. In conclusion, we verified that TMEM220-AS1 as a novel tumor suppressor and regulates HCC through miR-484/MAGI1 axis.

Materials And Methods

Collection of clinical samples

From 2016 to 2018, 50 paired fresh liver tumor and adjacent normal tissues were harvested in Zhongnan University Affiliated Xiangya Second Hospital. We snap-frozen these tissues at -80°C. All included subjects offered an informed consent and the research got approval from the Institutional Review Board of Zhongnan University Affiliated Xiangya Second Hospital.

Cell culture

HB611, HHCC, H-97, HuH-7, Li-7, and LO2 cell line were acquiredfrom the American Type Culture Collection (ATCC, Manassas VA, USA) and the Cell Bank of Chinese Academy of Science (Shanghai, China).The human immortalized liver LO2 cells were cultured in Dulbecco's modified Eagle's medium (DMEM; Gibco, USA). We cultured HCC cells in Dulbecco's modified Eagle's medium (DMEM) with high glucose concentration (25 mM), 1% of penicillin-streptomycin, 10% of fetal bovine serum (FBS), and maintained them in a 5% CO_2 humidified incubator.

Cell transfection

From BioVector NTCC Inc., Guangzhou, China, we purchased plasmid vector PLKO.1-puro. Through chemical synthesis, we designed the related TMEM220-AS1 short hairpin RNA(shRNA) sequences and its negative control. These synthetic related sequences were inserted into PLKO.1-puro vector. From RIBOBIO, Guangzhou, China, we purchased the microRNA mimics and its inhibitor. We cultured the cells for 24 h before transfection. Then, using Lipofectamine 3000 Transfection Reagent (Invitrogen, Carlsbad, CA, USA), we transfected the cells transiently with corresponding vector, during which we referred to the manufacturer's instructions. We harvested cells that were transfected with corresponding vector and

operated quantitative real-time polymerase chain reaction(qRT-PCR) after 48 h. Each experiment was carried out three times.

RNA isolation and qRT-PCR

With TRIzol reagent (Invitrogen, Carlsbad, CA, USA), total RNA from cells samples was extracted. Referring to the manufacturer's instructions, RNA was reverse transcribed via PrimerScript RT-PCR kit (Takara). The RNA level was determined using qRT-PCR analysis via TaqMan MicroRNA Assay Kit (Applied Biosystems). We measured their relative level of predicted targets in triplicate on an ABI 7500 real-time PCR machine (Applied Biosystems). U6 or β-actin was used as reference gene to normalize the expression levels of miRNA or mRNA. The delta Ct method was used to calculate the relative expression. Primers using in this study were shown in **Supplementary Table 1**.

Cell proliferation, invasion, cycle and apoptosis detection

These methods are shown in the **Supplementary Methods**.

Western blot evaluation

We prepared total cell lysates in a 1× sodium dodecyl sulfate buffer. Afterwards, we separated protein with sodium dodecyl sulfate-polyacrylamide gel electrophoresis, and onto nitrocellulose membranes total protein was transferred. Then, with 5% non-fat milk the membrane was blocked and with primary antibodies it was cultured at 4 °C overnight. After incubating with antibodies which is specific for BMI-1, E-cadherin, vimentin andsnail, the blots shared incubation with goat anti-rabbit secondary antibody (Abcam, Hong Kong, China) and via enhancedchemiluminescence they were visualized. Each experiment was carried out three times.

RNA fluorescent in situ hybridization (FISH)

With Ribo™ Fluorescent in Situ Hybridization Kit (Ribobio Company, China), FISH assay was implemented. TMEM220-AS1 probe was labeled with FITCfluorescent dye, the design and synthesis were implemented by Ribobio Company. RNA FISH were implemented utilizing fluorescent in situ hybridization kit (RiboBio)following the manufacturer’s instructions. With a confocal laser-scanning microscope (Leica, Germany), fluorescence detection was implemented.

RIP assay

Following the product specifications, we adopted the EZ-magna RIP kit (Millipore, United States) to carry out the RIP assay. We collected the HB611 and HuH-7 cells and lysed them in a full RIP lysis buffer. We incubated cell extracts with RIP buffer which contains magnetic beads conjugated to human AGO2 antibodies (ab32381, abcam, Cambridge, United Kingdom), and we used the IgG antibody (ab6702, abcam, Cambridge, United Kingdom) as controls. We incubated the samples with protease K and we oscillated them for digesting the protein and isolating the immunoprecipitated RNA. Via a NanoDrop

spectrophotometer, we measured the concentration of RNA and performed real-time PCR analysis of the purified RNA.

Dual luciferase reporter gene assay

First, we manufactured TMEM220-AS1 Wt and MAGI1 Wt. In brief, TMEM220-AS1 and MAGI1 fragments containing miR-484 bindingsites were amplified by PCR and cloned into the downstreamof luciferase reporter gene in pmirGLO vector, which werenamed TMEM220-AS1Wt and MAGI1 Wt.Usingthe Quickchange XL Site-Directed Mutagenesis Kit (Stratagene), we generated TMEM220-AS1 Mut and MAGI1 Mut (mutations within the binding sites). With TMEM220-AS1 Wt or TMEM220-AS1 Mut as well as MAGI1 Wt or MAGI1 Mut, MiR-NC and miR-484 mimics were co-transfected into HEK293T cells, respectively. Cells were harvested after 48 h of transfection and we utilized the Dual-Luciferase Reporter Assay System (Promega, Madison, WI, USA) to perform luciferase assay.

Immunochemistry

To detect Ki67 staining in tumor tissue samples, sections of 5 μm were cut. After series of dewaxing and hydration, the slides were rinsed in PBS, followed by boiling in 10 mM of sodium citrate when pH was 6. Then, the slides were incubated in 3% of H_2O_2 for 25 minutes to remove the horseradish peroxidase. The slides were blocked with 10% of BSA after washing with 1 × PBS for three times, followed by incubation for primary anti-Ki67 antibody (ab92742) at 4°C overnight. The slides were incubated with a second antibody labeled by HRP (rabbit) at room temperature for 45 minutes and with 3,3'-diaminobenzidine tetrahydrochloride (DAB) the immunoreactivity was visualized the next day. Finally, the slides were dehydrated and mounted with neutral gum.

Tumor xenograft implantation in nude mice

We divided six-week-old nude mice into two groups (3 mice per group) randomly, cultured them with continuous access to sterile food and water in pathogen-free sterile conditions. To establish the HCC xenograft model, we subcutaneously injected HuH-7 cells into nude mice. We monitored tumor growth every week and calculated it as equation: Volume = (Length) × $(Width)^2/2$.The study was approved by the Ethics Committee of Zhongnan University Affiliated Xiangya Second Hospital,, and experiments were performed following the NIH guidelines on animal welfare.

Statistical analysis

For normally distributed data with equal variance, the difference was evaluated by 2-tailed Student t test (2-group comparisons) or ANOVA followed by the post hoc Bonferroni test (multigroup comparisons) as appropriate. For nonnormally distributed data or data with unequal variances, the difference was evaluated by a nonparametric Mann-Whitney U test (2-group comparisons) or the Kruskal-Wallis test followed by the post hoc Bonferroni test (multigroup comparisons). The standard we used to determine statistical significance was that $P<0.05$. We carried out all tests via SPSS 22.0 (SPSS, Chicago, IL, USA).

Results

TMEM220-AS1 expression is decreased in HCC tissues and cell lines

Through the analysis of TCGA database, we found that TMEM220-AS1 was significantly lower in HCC tissues than in normal tissues (**Figure 1A**). Secondly, the expression level of TMEM220-AS1 in □+□ period was lower than that in□+□ period (**Figure 1B**).TMEM220 - AS1 expression amount in deadcases was lower than that in the alivecases (**Figure 1C**). We then verified this result in 50 HCC tissues and adjacent nontumorous tissues. Revealed by qRT-PCR assays, TMEM220-AS1 levels were significantly lower in HCC tissues than that in paired adjacent normal liver tissues (**Figure 1D**). We detected mRNA level of TMEM220-AS1 in 6 cell lines, which included one normal cell line (LO2) and 5 HCC cell lines (HB611, HHCC, H-97, HuH-7, and Li-7). Similarly, lower TMEM220-AS1 levels were showed in HCC cells rather than normal liver cells (**Figure 1E**). Data from the TCGA database showed that the overall survival rate of patients with low TMEM220- AS1 level was lower than that of patients with high TMEM220- AS1 level (**Figure 1F**).

TMEM220-AS1 inhibits proliferation and cell cycle of HCC cells, but promotes cell apoptosis of HCC cells

Two shRNAs targeting different sites of TMEM220-AS1 mRNA were adopted to knock TMEM220-AS1 down in HuH-7 cells (**Figure 2A**). Via a TMEM220-AS1-overexpressing vector, we also conducted TMEM220-AS1 overexpression in HB611 cells (**Figure 2A**). CCK-8 demonstrated that TMEM220-AS1 knockdown significantly promoted proliferation in HuH-7 cells, overexpression of TMEM220-AS1 greatly suppressed proliferation in HB61 cells (**Figure 2B**). Similar promotional effects of TMEM220-AS1 on HCC proliferation was also demonstrated by EdU assays **(Figure 2C**). In **Figure 2D**, proportion of the cell cycle S phase was increased by TMEM220-AS1 shRNA, while it was decreased by TMEM220-AS1 overexpression. Additionally, TMEM220-AS1elevatedthe apoptotic rate of HB611 cells, while, TMEM220-AS1 knockdown greatly suppressedthe apoptosis of HuH-7 cells **(Figure 2E)**.

TMEM220-AS1 inhibits cell invasion and EMT of HCC cells

Whether TMEM220-AS1 regulated invasion of HCC cells was further determined. Via transwell assay, the invasive ability of HCC cells was identified. Inhibited cell invasion was observed in HB611 cells which transfected with TMEM220-AS1-overexpressing vector.Contrarily, TMEM220-AS1 knockdown increased cell invasion (**Figure 3A**). Whether TMEM220-AS1 regulated EMT of HCC cells was further determined. We utilized qRT-PCR and western blot assay to observe the expression of EMT markers. E-cadherin expression was decreased while snail and vimentin expression were increased by TMEM220-AS1 knockdown in HCC cells (**Figure 3B, C**).

TMEM220-AS1 is targeted by miR-484

Biological effects and potential molecular roles of lncRNA associate closely with itssubcellular localization[16]. We performed nucleocytoplasmic separation experiment to detect the subcellular distribution of TMEM220-AS1. It was found that most of TMEM220-AS1 concentratedin the cytoplasm,

with minority in the nucleus (**Figure 4A**). Moreover, it was also confirmed by RNA-FISH assay (**Figure 4B**). To exactly uncover the underlying mechanisms of TMEM220-AS1 function, we searchedits potential targets using LncBase Experimental v.2.Bioinformatics analysis shows thatTMEM220-AS1 is targeted by miR-484. We showed the binding sites of wild-type (TMEM220-AS1 Wt) and mutant-type (TMEM220-AS1 Mut) in **Figure 4C**. Dual luciferase reporter assays in HEK293T cells demonstrated that luciferase activity was significantly reduced by TMEM220-AS1 Wt and miR-484 mimics co-transfection(**Figure 4D**). Via RIP assay, we further validated the interaction between miR-484 and TMEM220-AS1.We found thatboth TMEM220-AS1 and miR-484 are enrichedin the AGO2-containing miRNA ribonucleoprotein complexes (**Figure 4E**). Consistently, both TCGA database and our samples showed that miR-484 expression in HCC tumor samples was higher than negative control samples (**Figure 4F, H**). Moreover, TMEM220-AS1 expression levels was negatively correlated with miR-484 expression in HCC samples, both in TCGA database and our samples (**Figure4G, I**). Altogether, the above results proved that TMEM220-AS1 was targeted by miR-484.

TMEM220-AS1 regulates the miR-484 target gene, MAGI1

Target genes of miR-484 were screened out through MIRDB,and MAGI1 with the highest score was chosen for further research. We showed the binding sites of wild-type (MAGI1 Wt) and mutant-type (MAGI1Mut) (**Figure 5A**). Dual luciferase reporter assays demonstrated that luciferase activity was significantly reduced by MAGI1Wt and miR-484 mimics co-transfection (**Figure 5B**). Then, both the TCGA database and our samples showed that MAGI1 gene expression in HCC samples was decreased compared with negative control samples (**Figure 5C, F**). Moreover, MAGI1 expression level was negatively correlated with miR-484 expression in HCC samples (**Figure 5D, G**), but it was positively correlated with TMEM220-AS1 expression in HCC samples, according to TCGA database and our samples (**Figure 5E, H**). Altogether, MAGI1 is indicated to be a target gene of miR-484.

Next, we used western blot assay to investigate whether TMEM220-AS1 can modulate the expression of MAGI1 in HCC cells via miR-484. Results showed that MAGI1 expression level was inhibited by sh-TMEM220-AS1 and miR-484 mimics (**Figure 5I, J**). While, MAGI1 expression level was promoted by TMEM220-AS1 overexpression and miR-484 inhibitor (**Figure 5I, J**). Knocking miR-484 down partially reversed the MAGI1 inhibition due to the silence of TMEM220-AS1 in HuH-7 cells (**Figure 5K**).The results indicated thatTMEM220-AS1 modulated MAGI1 expression via miR-484-dependent manner in HCC cells. The transfection efficiency of miR-484 mimics and miR-484 inhibitor was shown in **Supplementary Figure 1**.

TMEM220-AS1/miR-484 axis regulates behaviors of HCC cells

Subsequently, we explored the effect of TMEM220-AS1/miR-484 axis on HCC. We transfected HuH-7 cells and divided them into sh-NC+inh-NC group, sh-TMEM220-AS1#1(shRNA#1)+inh-NC group, sh-NC+miR-484 inh group, and sh-TMEM220-AS1#1(shRNA#1)+miR-484 inh group. Firstly, EdU assay exhibited that the cell proliferation was increased by silencing TMEM220-AS1, but it was decreased by miR-484 inhibitor, and miR-484 inhibitor treatment reversed the promoting effect of TMEM220-AS1 silence on cell

proliferation (**Figure 6A**). Next, Cell S-phase proportion was increased by silencing TMEM220-AS1, while miR-484 inhibitor decreased cell S-phase proportion. And the influence of TMEM220-AS1 shRNA on cell cycle could be reversed by co-transfection of miR-484 inhibitor (**Figure 6B**). Besides, miR-484 inhibitor promoted cell apoptosis. Knocking TMEM220-AS1 down inhibited cell apoptosis, but the influence of knocking TMEM220-AS1 down on cell apoptosis could be reversed by co-transfection of miR-484 inhibitor (**Figure 6C**).Last, the cell invasion was increased by silencing TMEM220-AS1, but it was decreased by miR-484 inhibitor. Moreover, miR-484 inhibitor treatment reversed the promoting effect of TMEM220-AS1 silence on cell invasion (**Figure 6D**).

TMEM220-AS1 shRNA promoted growth and metastasis of HCC in vivo

Furtherly, we generated xenograft models to verify our findings. TMEM220-AS1 knockdown was found greatly promoted tumor proliferation in vivo (**Figure 7A-C**). We displayed tumors collected from mice in **Figure 7A**. Tumor growth of sh-NC group was lower than that in the sh-TMEM220-AS1 treatment group both in volume and weight (**Figure 7B, C**). qRT-PCR and western blot assay pointed out that TMEM220-AS1 knockdown decreased MAGI1 expression *in vivo*, but it promoted EMT of HCC cells (**Figure 7D, E**). The result of immunohistochemistry also showed that knockdown of TMEM220-AS1 inhibited MAGI1 expression, but it increased ki67 expression in xenograft tumors tissues (**Figure 7F**). Moreover, TMEM220-AS1 knockdown in pulmonary metastasis models greatly increased the incidence of pulmonary metastasis (**Figure 7G**). In a word, TMEM220-AS1 inhibited HCC growth and metastasis *in vivo*.

Discussion

Hepatocellular carcinoma is a frequent malignant tumor of the digestive system, with occurrence associated with unrestricted proliferation of hepatocytes[17]. Therefore, any cause of hepatocyte proliferation may lead to the occurrence of HCC. In recent years, lncRNAs have become a focus of tumor-related research, and there are a lot of evidences that they can participate in the modulation of cancer cell migration, proliferation and apoptosis[18-21]. Here, TMEM220-AS1 was selectedby analyzing the TCGA database which was poorly expressed in HCC samples and was associated with clinical staging and survival prognosis. Then, we verified the low expression of TMEM220-AS1 with a large population-based samples (n=50), and the results of subsequent cell function experiments showed that the down-regulation of TMEM220-AS1 promoted the cell proliferation, cycle, invasion and EMT process, while the cell apoptosis was inhibited. Next, we studied the specific mechanism of TMEM220-AS1 in HCC.

It was indicated that lncRNAs can interact with miRNAs and regulate target mRNAs[22, 23]. For example, AGAP2-AS1promotes ANXA11 expression by sponging miR-16-5p and promotes proliferation and metastasis in HCC[24]. Another article showed that the growth and epithelial-to-mesenchymal transition phenotype were regulated by LINC01287/miR-298/STAT3 feedback loop in HCC cells[25]. Also, the migration and invasion of HCC cells were promoted by LncRNA n335586/miR-924/CKMT1A axis[26]. In our research, LncBase Experimental v.2 was adopted to predict miRNA which might bind to TMEM220-AS1, and the results showed that only miR-484 may be associated with TMEM220-AS1. Moreover, miR-

484 has been reported to promote non-small-cell lung cancer[27] and HCC[28] progression. Subsequent results also confirmed that miR-484 inhibitor curbed the invasion, proliferation and cell cycle of HuH-7 cells and promoted the apoptosis of HuH-7 cells. Moreover, miR-484 inhibitor can partially reverse the effects of TMEM220-AS1 shRNA on the proliferation, invasion, cell cycle and apoptosis of HCC cells.

The downstream target genes of miR-484 was predicted using MIRDB, MAGI1 with the highest score was chosen to forsubsequentresearch. Some studies indicated that, in estrogen receptor positive breast cancer, MAGI1 is a new potential tumor suppressor gene[29].Via the Wnt/β-Catenin and PTEN/AKT signaling pathways, MAGI1 silencing inhibited apoptosis of glioma cells and promoted the proliferation[30]. Moreover, via regulating PTEN, MAGI1 curbed invasion and migration of HCC[31].Our study confirmed that MAGI1 was the downstream target gene of miR-484, and TMEM220-AS1 released MAGI1 through competitive binding of miR-484, thereby regulating the progression of HCC.

Conclusion

In conclusion, TMEM220-AS1 acted as a tumor suppressor gene and inhibited cell cycle, invasion,proliferation and EMT of HCC cells. Moreover, TMEM220-AS1 promoted cell apoptosis of HCC cells. And TMEM220-AS1 inhibited HCC progression through miR-484/MAGI1 axis.

Declarations

Ethics approval and consent to participate

All included subjects offered an informed consent and the research got approval from the Institutional Review Board of Zhongnan University Affiliated Xiangya Second Hospital. And all animal experiments were performed following the NIH guidelines on animal welfare.

Consent for publication

Not applicable.

Availability of data and materials

The datasets used/or analysed during the current study are available from the corresponding author on reasonable request.

Competing interests

The authors declare that they have no competing interests.

Funding

This work was supported by Guangxi Universities and Young Teachers Research Basic Ability Improvement Project [grant No. 2020KY13020] and Innovation Project of Guangxi Graduate Education

[grant No. JGY2020166].

Author's contributions

Song Cao and **Jiequn Li** designed the study. **Cong Cao**, **Jun Li** and **Guangzhi Li** performed the experiments. **Zhihua Deng** and **Bing Huang** collected and analyzed the data. **Jing Yang** instructed data analysis, figure production and manuscript writing. **Cong Cao** drafted the manuscript. **Song Cao** revised the final manuscript.

Acknowledgements

Not applicable.

References

1. Nakagawa H, Fujita M, Fujimoto A: **Genome sequencing analysis of liver cancer for precision medicine.***Semin Cancer Biol* 2019, **55:**120-127.
2. Anwanwan D, Singh SK, Singh S, Saikam V, Singh R: **Challenges in liver cancer and possible treatment approaches.***Biochim Biophys Acta Rev Cancer* 2020, **1873:**188314.
3. Rahmani J, Kord Varkaneh H, Kontogiannis V, Ryan PM, Bawadi H, Fatahi S, Zhang Y: **Waist Circumference and Risk of Liver Cancer: A Systematic Review and Meta-Analysis of over 2 Million Cohort Study Participants.***Liver Cancer* 2020, **9:**6-14.
4. Ringelhan M, McKeating JA, Protzer U: **Viral hepatitis and liver cancer.***Philos Trans R Soc Lond B Biol Sci* 2017, **372**.
5. Gailhouste L, Liew LC, Yasukawa K, Hatada I, Tanaka Y, Nakagama H, Ochiya T: **Differentiation Therapy by Epigenetic Reconditioning Exerts Antitumor Effects on Liver Cancer Cells.***Mol Ther* 2018, **26:**1840-1854.
6. Momin BR, Pinheiro PS, Carreira H, Li C, Weir HK: **Liver cancer survival in the United States by race and stage (2001-2009): Findings from the CONCORD-2 study.***Cancer* 2017, **123 Suppl 24:**5059-5078.
7. Ryerson AB, Eheman CR, Altekruse SF, Ward JW, Jemal A, Sherman RL, Henley SJ, Holtzman D, Lake A, Noone AM, et al: **Annual Report to the Nation on the Status of Cancer, 1975-2012, featuring the increasing incidence of liver cancer.***Cancer* 2016, **122:**1312-1337.
8. Kim Y, Ejaz A, Tayal A, Spolverato G, Bridges JF, Anders RA, Pawlik TM: **Temporal trends in population-based death rates associated with chronic liver disease and liver cancer in the United States over the last 30 years.***Cancer* 2014, **120:**3058-3065.
9. Chi Y, Gong Z, Xin H, Wang Z, Liu Z: **Long noncoding RNA lncARSR promotes nonalcoholic fatty liver disease and hepatocellular carcinoma by promoting YAP1 and activating the IRS2/AKT pathway.***J Transl Med* 2020, **18:**126.
10. Zhou Y, Huang Y, Hu K, Zhang Z, Yang J, Wang Z: **HIF1A activates the transcription of lncRNA RAET1K to modulate hypoxia-induced glycolysis in hepatocellular carcinoma cells via miR-100-**

5p.*Cell Death Dis* 2020, **11:**176.

11. Lian Y, Xiong F, Yang L, Bo H, Gong Z, Wang Y, Wei F, Tang Y, Li X, Liao Q, et al: **Long noncoding RNA AFAP1-AS1 acts as a competing endogenous RNA of miR-423-5p to facilitate nasopharyngeal carcinoma metastasis through regulating the Rho/Rac pathway.***J Exp Clin Cancer Res* 2018, **37:**253.
12. Tichon A, Perry RB, Stojic L, Ulitsky I: **SAM68 is required for regulation of Pumilio by the NORAD long noncoding RNA.***Genes Dev* 2018, **32:**70-78.
13. Jin J, Xu H, Li W, Xu X, Liu H, Wei F: **LINC00346 Acts as a Competing Endogenous RNA Regulating Development of Hepatocellular Carcinoma via Modulating CDK1/CCNB1 Axis.***Front Bioeng Biotechnol* 2020, **8:**54.
14. Zhang W, Liu Y, Fu Y, Han W, Xu H, Wen L, Deng Y, Liu K: **Long non-coding RNA LINC00160 functions as a decoy of microRNA-132 to mediate autophagy and drug resistance in hepatocellular carcinoma via inhibition of PIK3R3.***Cancer Lett* 2020, **478:**22-33.
15. Guo T, Gong C, Wu P, Battaglia-Hsu SF, Feng J, Liu P, Wang H, Guo D, Yao Y, Chen B, et al: **LINC00662 promotes hepatocellular carcinoma progression via altering genomic methylation profiles.***Cell Death Differ* 2020.
16. Wen X, Gao L, Guo X, Li X, Huang X, Wang Y, Xu H, He R, Jia C, Liang F: **lncSLdb: a resource for long non-coding RNA subcellular localization.***Database (Oxford)* 2018, **2018:**1-6.
17. Jin L, He Y, Tang S, Huang S: **LncRNA GHET1 predicts poor prognosis in hepatocellular carcinoma and promotes cell proliferation by silencing KLF2.***J Cell Physiol* 2018, **233:**4726-4734.
18. Shang R, Wang M, Dai B, Du J, Wang J, Liu Z, Qu S, Yang X, Liu J, Xia C, et al: **Long noncoding RNA SLC2A1-AS1 regulates aerobic glycolysis and progression in hepatocellular carcinoma via inhibiting the STAT3/FOXM1/GLUT1 pathway.***Mol Oncol* 2020.
19. Nekvindova J, Mrkvicova A, Zubanova V, Vaculova AH, Anzenbacher P, Soucek P, Radova L, Slaby O, Kiss I, Vondracek J, et al: **Hepatocellular carcinoma: gene expression profiling and regulation of xenobiotic-metabolizing cytochromes P450.***Biochem Pharmacol* 2020**:**113912.
20. Wang J, Ding W, Xu Y, Tao E, Mo M, Xu W, Cai X, Chen X, Yuan J, Wu X: **Long non-coding RNA RHPN1-AS1 promotes tumorigenesis and metastasis of ovarian cancer by acting as a ceRNA against miR-596 and upregulating LETM1.***Aging (Albany NY)* 2020, **12**.
21. Chen Z, Pan T, Jiang D, Jin L, Geng Y, Feng X, Shen A, Zhang L: **The lncRNA-GAS5/miR-221-3p/DKK2 Axis Modulates ABCB1-Mediated Adriamycin Resistance of Breast Cancer via the Wnt/beta-Catenin Signaling Pathway.***Mol Ther Nucleic Acids* 2020, **19:**1434-1448.
22. Lyu K, Li Y, Xu Y, Yue H, Wen Y, Liu T, Chen S, Liu Q, Yang W, Zhu X, et al: **Using RNA sequencing to identify a putative lncRNA-associated ceRNA network in laryngeal squamous cell carcinoma.***RNA Biol* 2020.
23. Bo H, Liu Z, Zhu F, Zhou D, Tan Y, Zhu W, Fan L: **Long noncoding RNAs expression profile and long noncoding RNA-mediated competing endogenous RNA network in nonobstructive azoospermia patients.***Epigenomics* 2020.

24. Liu Z, Wang Y, Wang L, Yao B, Sun L, Liu R, Chen T, Niu Y, Tu K, Liu Q: **Long non-coding RNA AGAP2-AS1, functioning as a competitive endogenous RNA, upregulates ANXA11 expression by sponging miR-16-5p and promotes proliferation and metastasis in hepatocellular carcinoma.***J Exp Clin Cancer Res* 2019, **38:**194.
25. Mo Y, He L, Lai Z, Wan Z, Chen Q, Pan S, Li L, Li D, Huang J, Xue F, Che S: **LINC01287/miR-298/STAT3 feedback loop regulates growth and the epithelial-to-mesenchymal transition phenotype in hepatocellular carcinoma cells.***J Exp Clin Cancer Res* 2018, **37:**149.
26. Fan H, Lv P, Mu T, Zhao X, Liu Y, Feng Y, Lv J, Liu M, Tang H: **LncRNA n335586/miR-924/CKMT1A axis contributes to cell migration and invasion in hepatocellular carcinoma cells.***Cancer Lett* 2018, **429:**89-99.
27. Li T, Ding ZL, Zheng YL, Wang W: **MiR-484 promotes non-small-cell lung cancer (NSCLC) progression through inhibiting Apaf-1 associated with the suppression of apoptosis.***Biomed Pharmacother* 2017, **96:**153-164.
28. Qiu L, Huang Y, Li Z, Dong X, Chen G, Xu H, Zeng Y, Cai Z, Liu X, Liu J: **Circular RNA profiling identifies circADAMTS13 as a miR-484 sponge which suppresses cell proliferation in hepatocellular carcinoma.***Mol Oncol* 2019, **13:**441-455.
29. Alday-Parejo B, Richard F, Worthmuller J, Rau T, Galvan JA, Desmedt C, Santamaria-Martinez A, Ruegg C: **MAGI1, a New Potential Tumor Suppressor Gene in Estrogen Receptor Positive Breast Cancer.***Cancers (Basel)* 2020, **12**.
30. Lu Y, Sun W, Zhang L, Li J: **Silencing Of MAGI1 Promotes The Proliferation And Inhibits Apoptosis Of Glioma Cells Via The Wnt/beta-Catenin And PTEN/AKT Signaling Pathways.***Onco Targets Ther* 2019, **12:**9639-9650.
31. Zhang G, Wang Z: **MAGI1 inhibits cancer cell migration and invasion of hepatocellular carcinoma via regulating PTEN.***Zhong Nan Da Xue Xue Bao Yi Xue Ban* 2011, **36:**381-385.

Figures

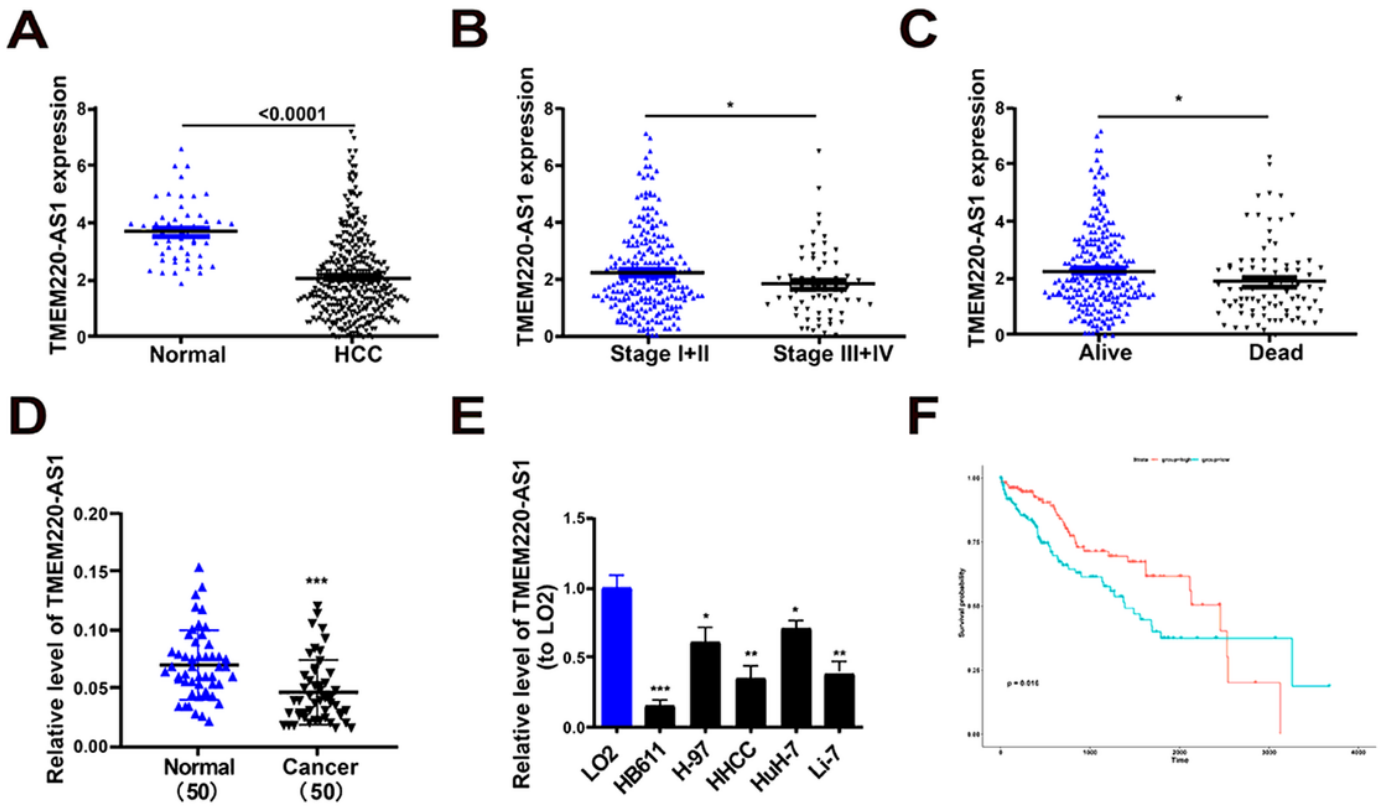

Figure 1

TMEM220-AS1 expression is down-regulated in HCC (A) TMEM220-AS1 expression in HCC samples and normal samples, from TCGA database. (B) TMEM220-AS1 expression in stage Ⅰ+Ⅱ and stage Ⅲ+Ⅳ, from TCGA database. (C) TMEM220-AS1 expression in alive samples and dead samples, from TCGA database. (D) TMEM220-AS1 expression in HCC tissues and paired adjacent normal tissues was analyzed by qRT-PCR. (E) TMEM220-AS1 expression in HCC cell lines and LO2 cell line was analyzed by qRT-PCR. (F) Kaplan-Meier curves of overall survival (OS) from TCGA database. Data represent the mean ± SD;*P <0.05, ** P <0.01, ***P < 0.001.

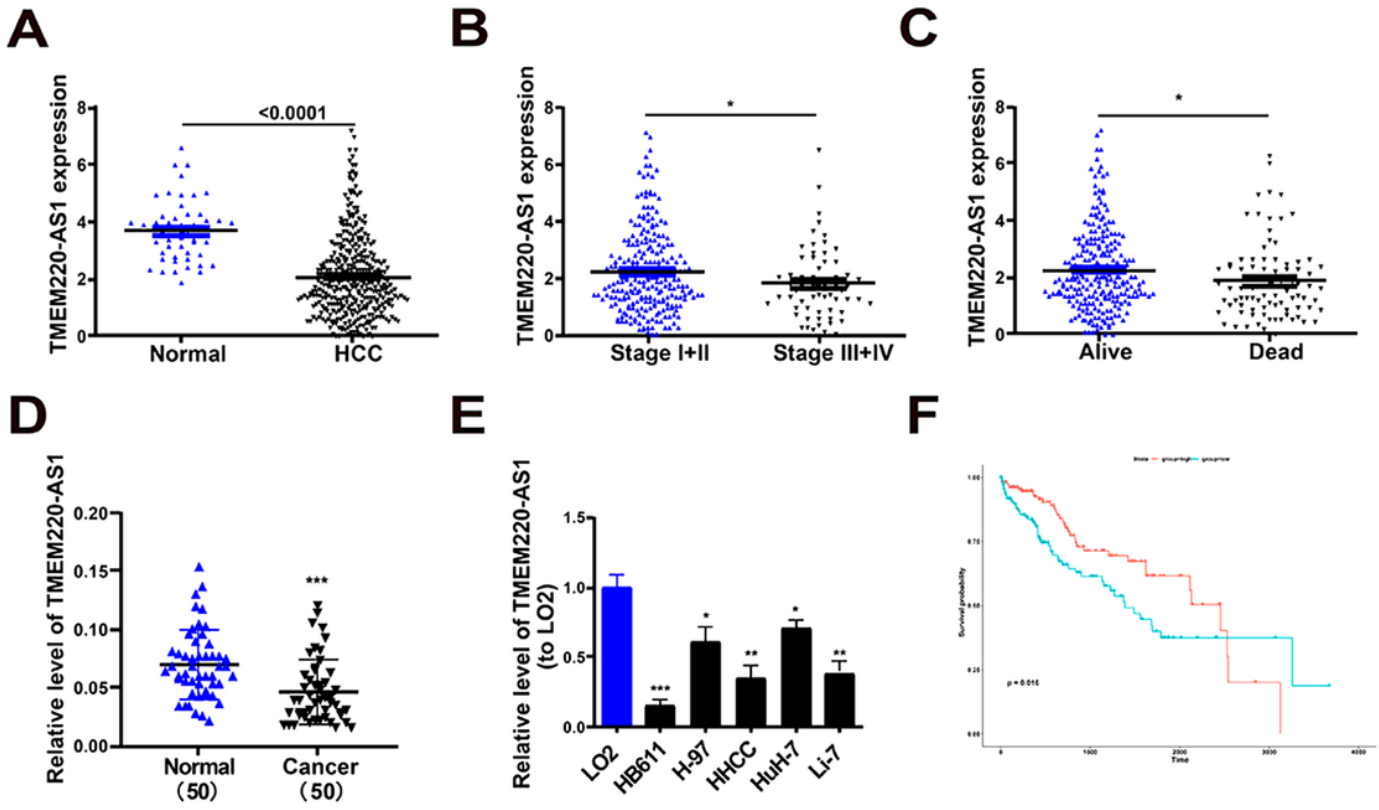

Figure 1

TMEM220-AS1 expression is down-regulated in HCC (A) TMEM220-AS1 expression in HCC samples and normal samples, from TCGA database. (B) TMEM220-AS1 expression in stage Ⅰ+Ⅱ and stage Ⅲ+Ⅳ, from TCGA database. (C) TMEM220-AS1 expression in alive samples and dead samples, from TCGA database. (D) TMEM220-AS1 expression in HCC tissues and paired adjacent normal tissues was analyzed by qRT-PCR. (E) TMEM220-AS1 expression in HCC cell lines and LO2 cell line was analyzed by qRT-PCR. (F) Kaplan-Meier curves of overall survival (OS) from TCGA database. Data represent the mean ± SD;*P <0.05, ** P <0.01, ***P < 0.001.

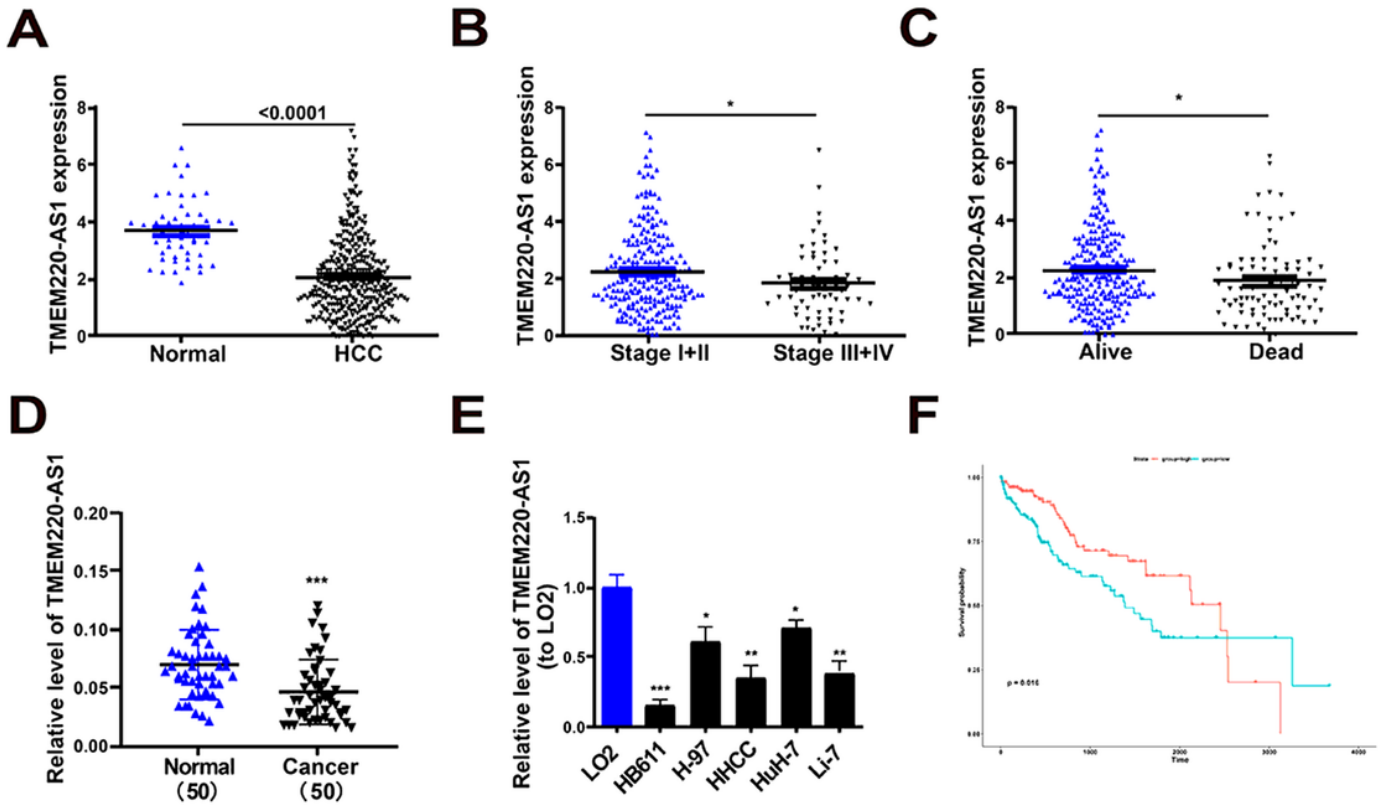

Figure 1

TMEM220-AS1 expression is down-regulated in HCC (A) TMEM220-AS1 expression in HCC samples and normal samples, from TCGA database. (B) TMEM220-AS1 expression in stage Ⅰ+Ⅱ and stage Ⅲ+Ⅳ, from TCGA database. (C) TMEM220-AS1 expression in alive samples and dead samples, from TCGA database. (D) TMEM220-AS1 expression in HCC tissues and paired adjacent normal tissues was analyzed by qRT-PCR. (E) TMEM220-AS1 expression in HCC cell lines and LO2 cell line was analyzed by qRT-PCR. (F) Kaplan-Meier curves of overall survival (OS) from TCGA database. Data represent the mean ± SD;*P <0.05, ** P <0.01, ***P < 0.001.

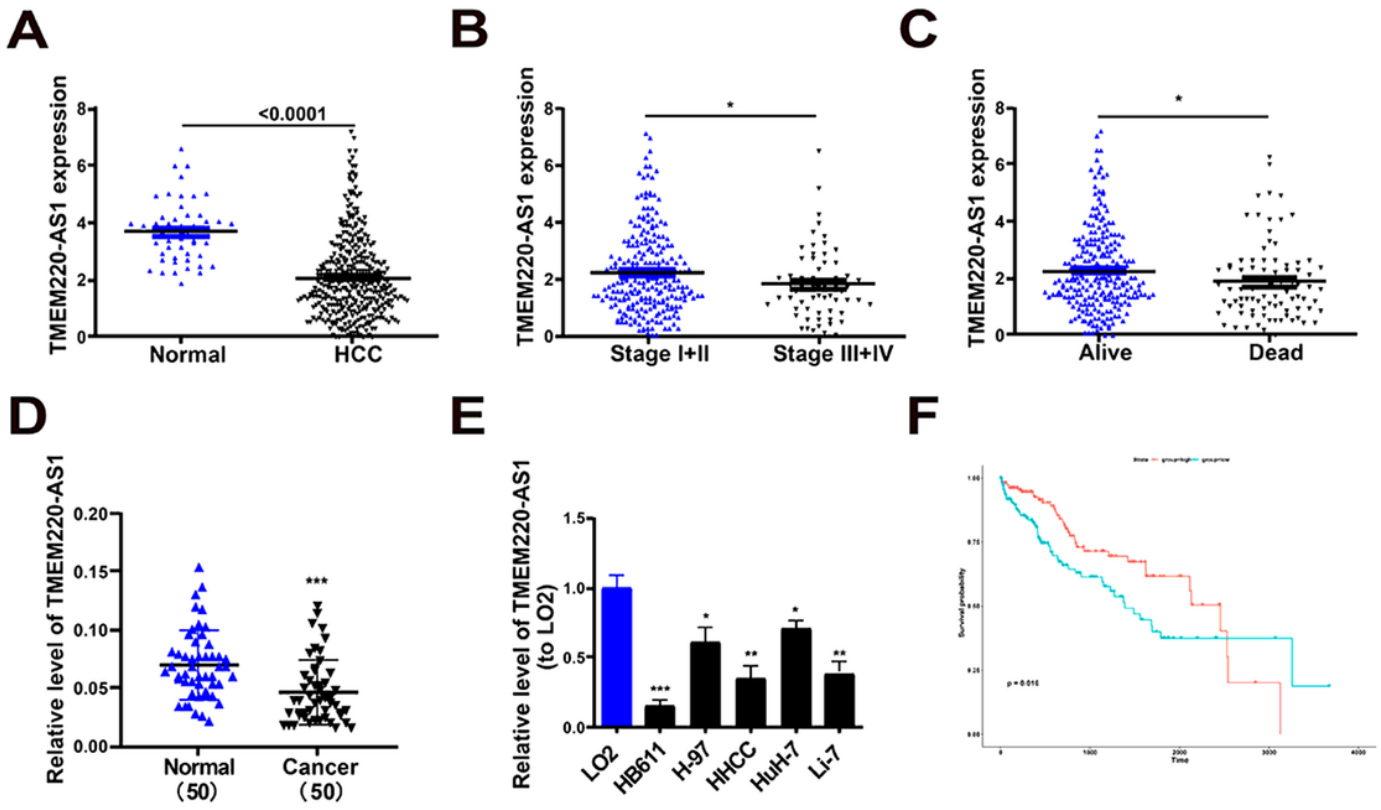

Figure 1

TMEM220-AS1 expression is down-regulated in HCC (A) TMEM220-AS1 expression in HCC samples and normal samples, from TCGA database. (B) TMEM220-AS1 expression in stage Ⅰ+Ⅱ and stage Ⅲ+Ⅳ, from TCGA database. (C) TMEM220-AS1 expression in alive samples and dead samples, from TCGA database. (D) TMEM220-AS1 expression in HCC tissues and paired adjacent normal tissues was analyzed by qRT-PCR. (E) TMEM220-AS1 expression in HCC cell lines and LO2 cell line was analyzed by qRT-PCR. (F) Kaplan-Meier curves of overall survival (OS) from TCGA database. Data represent the mean ± SD;*P <0.05, ** P <0.01, ***P < 0.001.

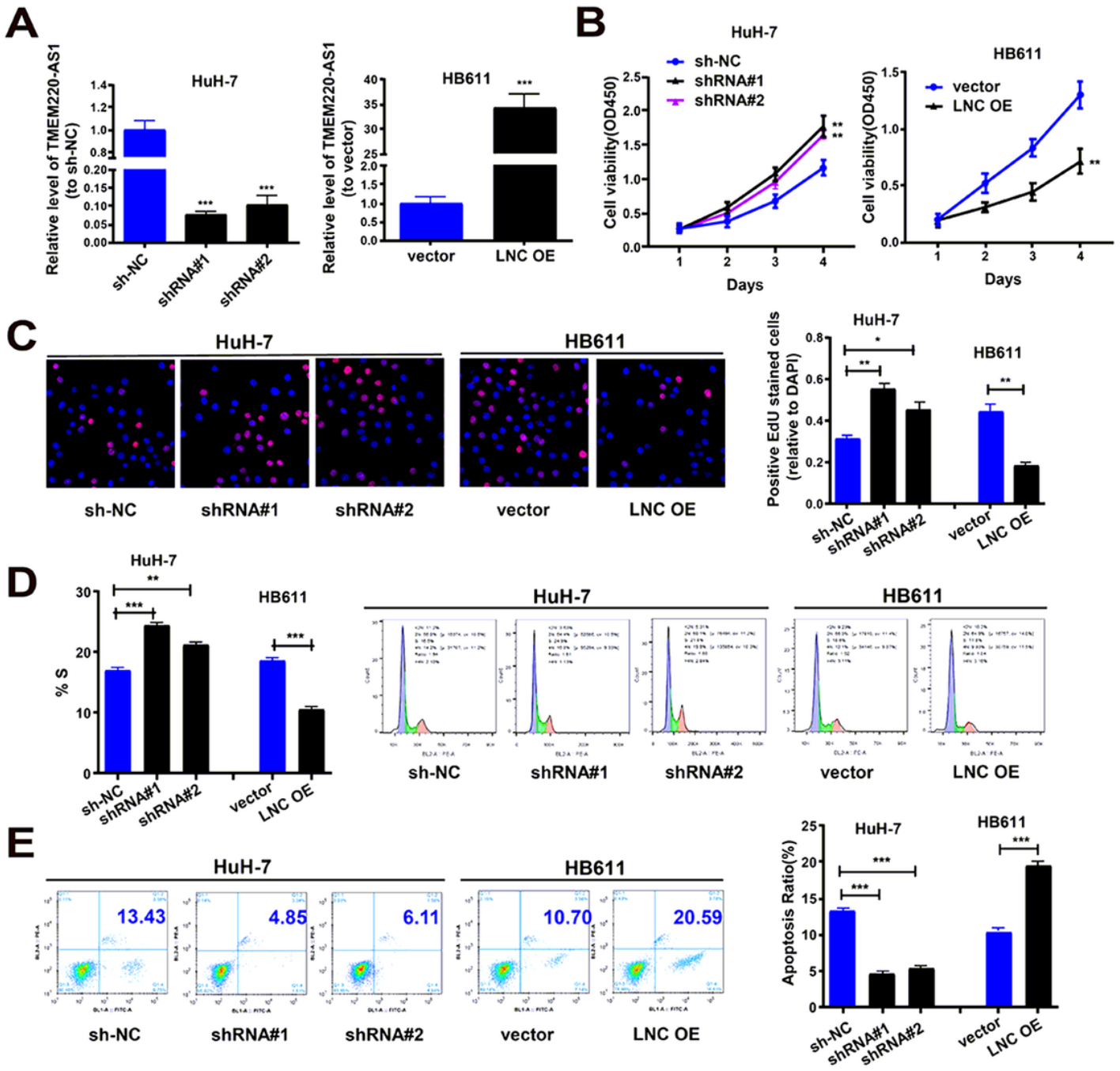

Figure 2

TMEM220-AS1 inhibits proliferation and cell cycle of HCC cells, but promotes cell apoptosis of HCC cells (A) Transfection efficiency of sh-TMEM220-AS1#1(shRNA#1), sh-TMEM220-AS1#2(shRNA#2) and TMEM220-AS1-overexpressing vector(LNC OE). (B) CCK-8 assay. (C) EdU assay. (D) Cell cycle. (E) Cell apoptosis. Data were presented asrepresent the mean ± SD of 3 independent experiments; *P <0.05, ** P <0.01, ***P < 0.001.

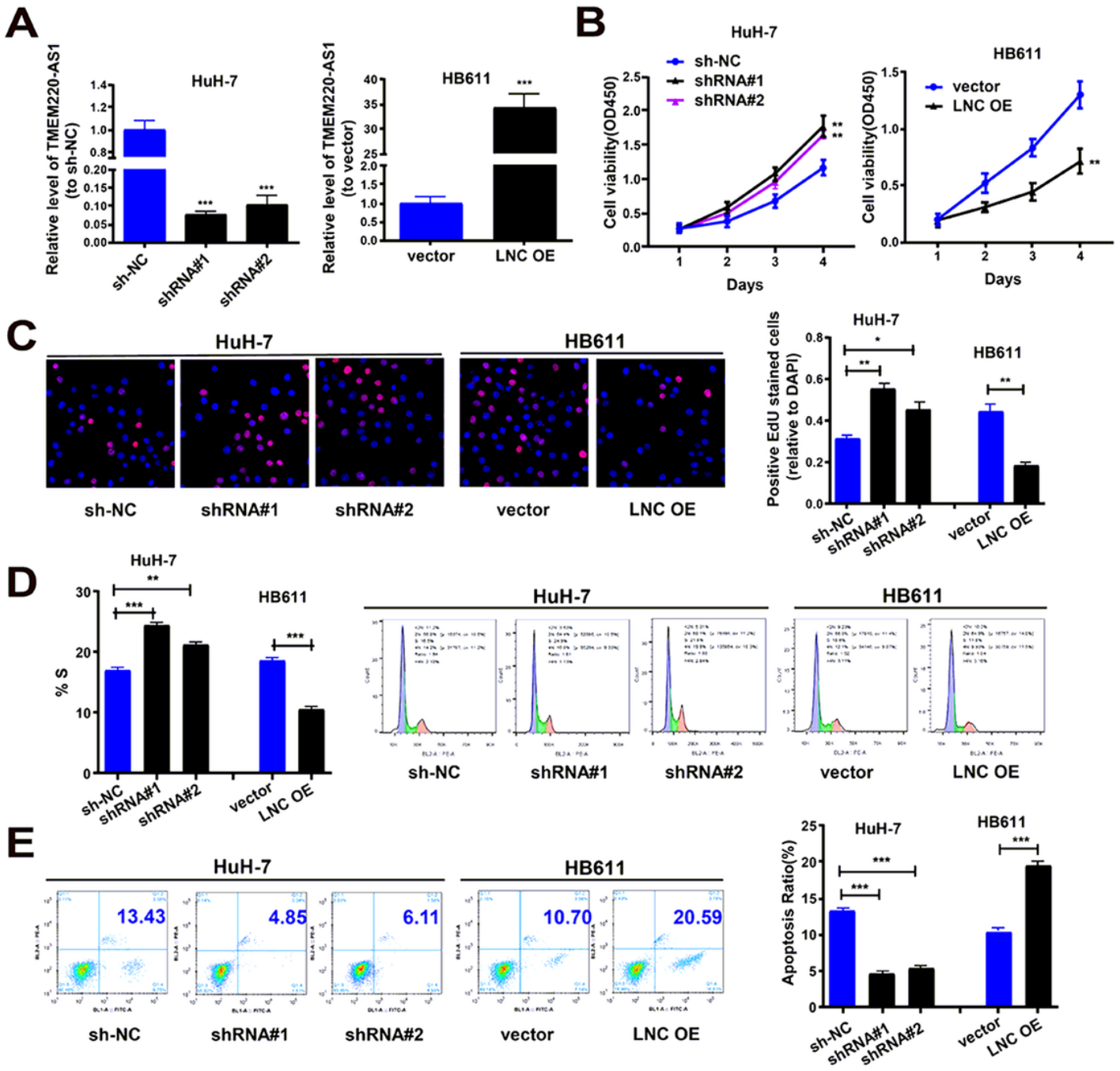

Figure 2

TMEM220-AS1 inhibits proliferation and cell cycle of HCC cells, but promotes cell apoptosis of HCC cells (A) Transfection efficiency of sh-TMEM220-AS1#1(shRNA#1), sh-TMEM220-AS1#2(shRNA#2) and TMEM220-AS1-overexpressing vector(LNC OE). (B) CCK-8 assay. (C) EdU assay. (D) Cell cycle. (E) Cell apoptosis. Data were presented asrepresent the mean ± SD of 3 independent experiments; *P <0.05, ** P <0.01, ***P < 0.001.

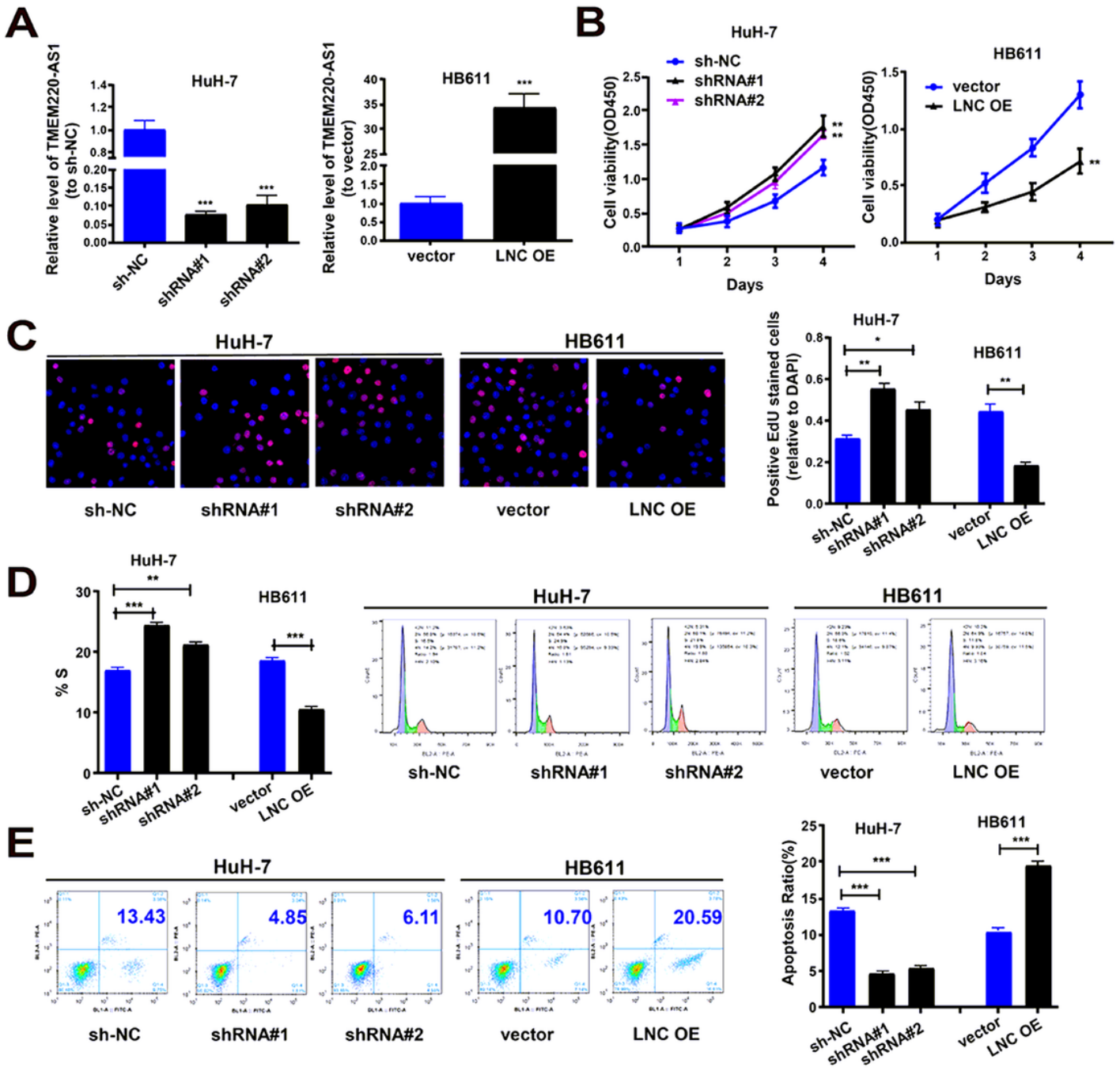

Figure 2

TMEM220-AS1 inhibits proliferation and cell cycle of HCC cells, but promotes cell apoptosis of HCC cells (A) Transfection efficiency of sh-TMEM220-AS1#1(shRNA#1), sh-TMEM220-AS1#2(shRNA#2) and TMEM220-AS1-overexpressing vector(LNC OE). (B) CCK-8 assay. (C) EdU assay. (D) Cell cycle. (E) Cell apoptosis. Data were presented asrepresent the mean ± SD of 3 independent experiments; *P <0.05, ** P <0.01, ***P < 0.001.

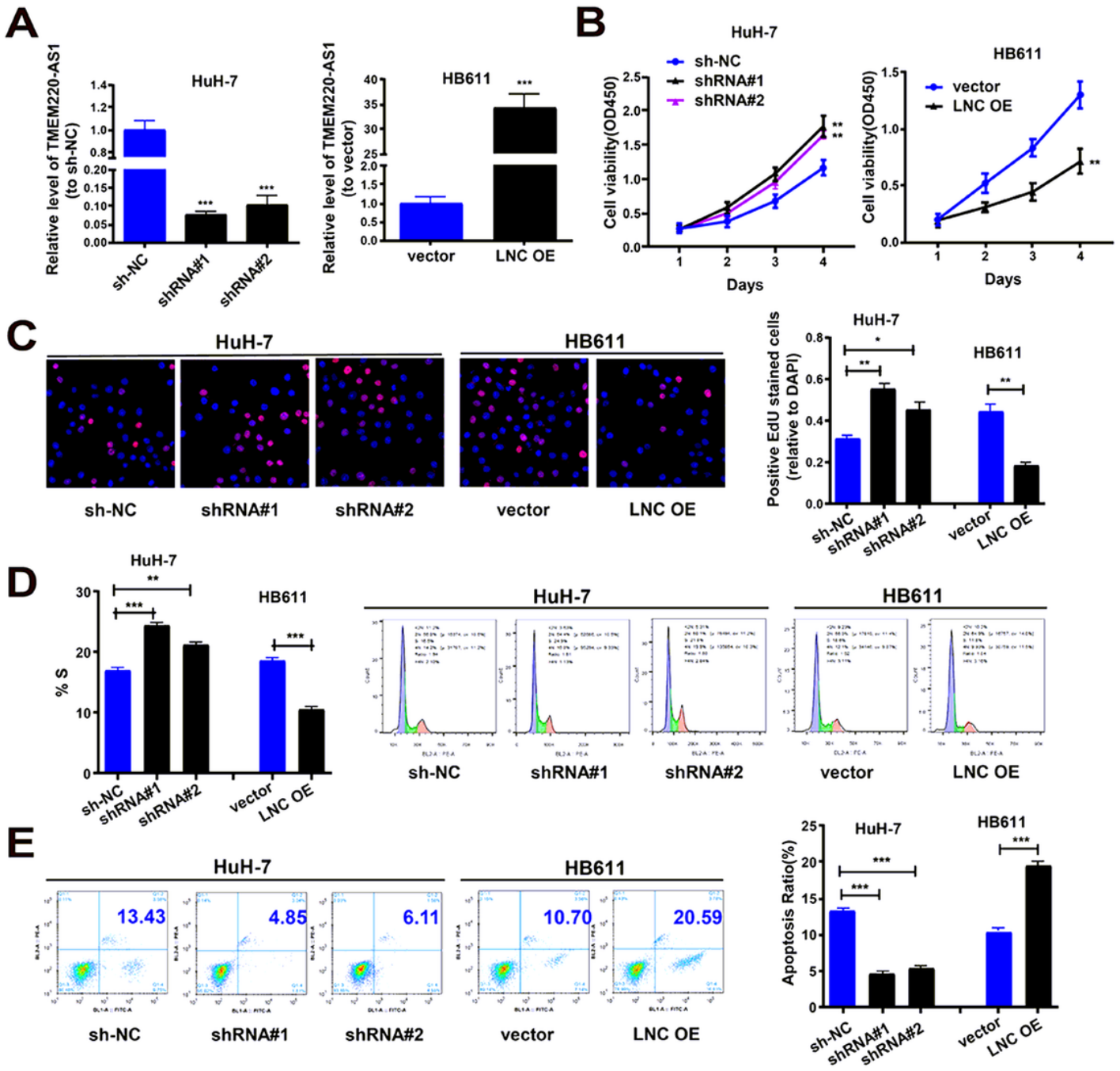

Figure 2

TMEM220-AS1 inhibits proliferation and cell cycle of HCC cells, but promotes cell apoptosis of HCC cells (A) Transfection efficiency of sh-TMEM220-AS1#1(shRNA#1), sh-TMEM220-AS1#2(shRNA#2) and TMEM220-AS1-overexpressing vector(LNC OE). (B) CCK-8 assay. (C) EdU assay. (D) Cell cycle. (E) Cell apoptosis. Data were presented asrepresent the mean ± SD of 3 independent experiments; *P <0.05, ** P <0.01, ***P < 0.001.

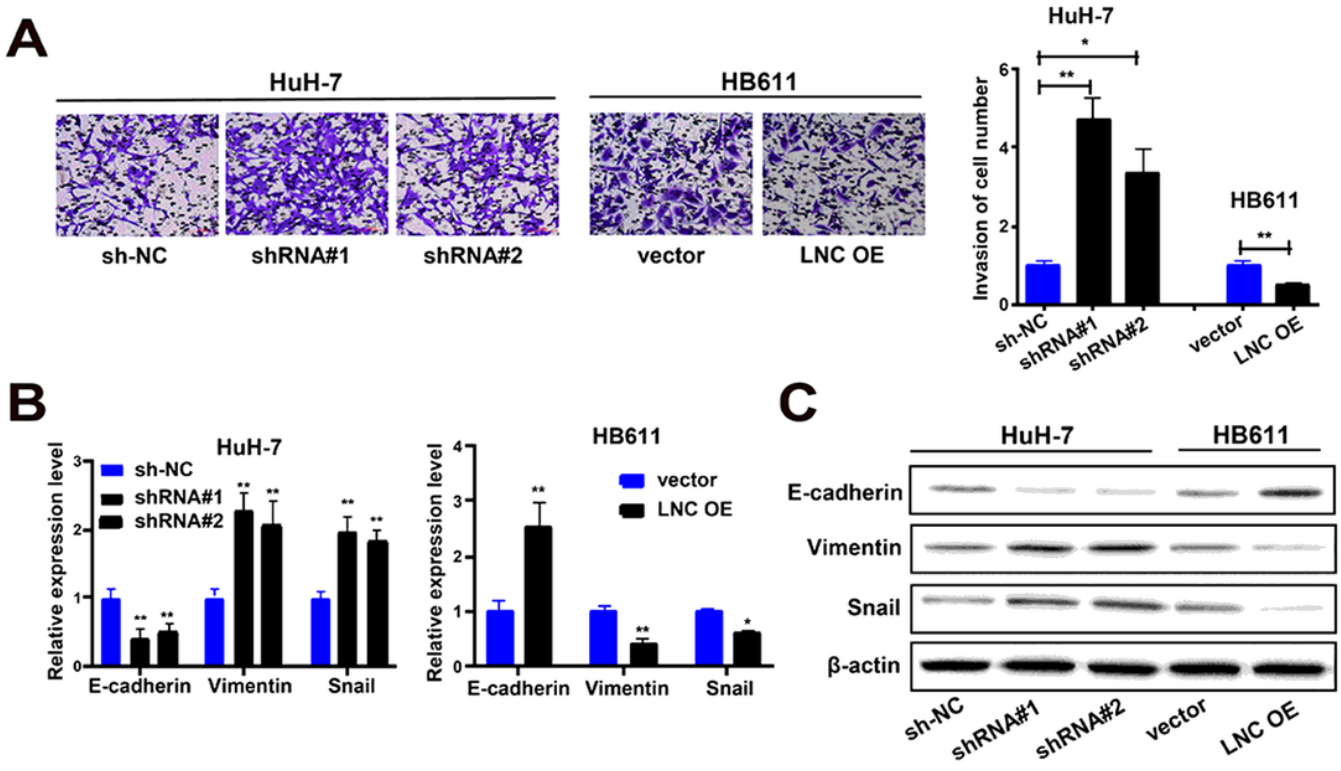

Figure 3

TMEM220-AS1 inhibits cell invasion and EMT of HCC cells (A) Cell invasion was determined using transwell assay. (B, C) The expression of EMT markers were determined using qRT-PCR and western blot assay. Data were presented asrepresent the mean ± SD of 3 independent experiments;*P <0.05, ** P <0.01.

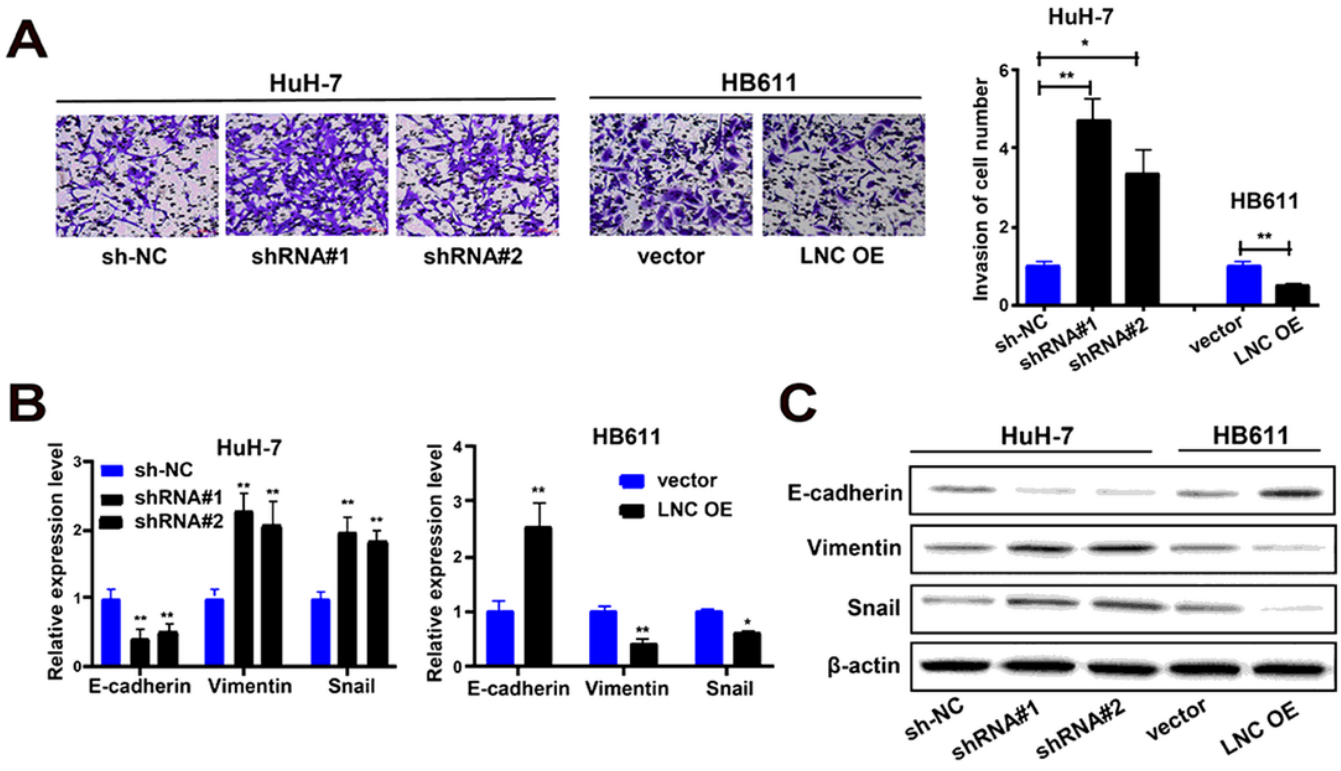

Figure 3

TMEM220-AS1 inhibits cell invasion and EMT of HCC cells (A) Cell invasion was determined using transwell assay. (B, C) The expression of EMT markers were determined using qRT-PCR and western blot assay. Data were presented asrepresent the mean ± SD of 3 independent experiments;*P <0.05, ** P <0.01.

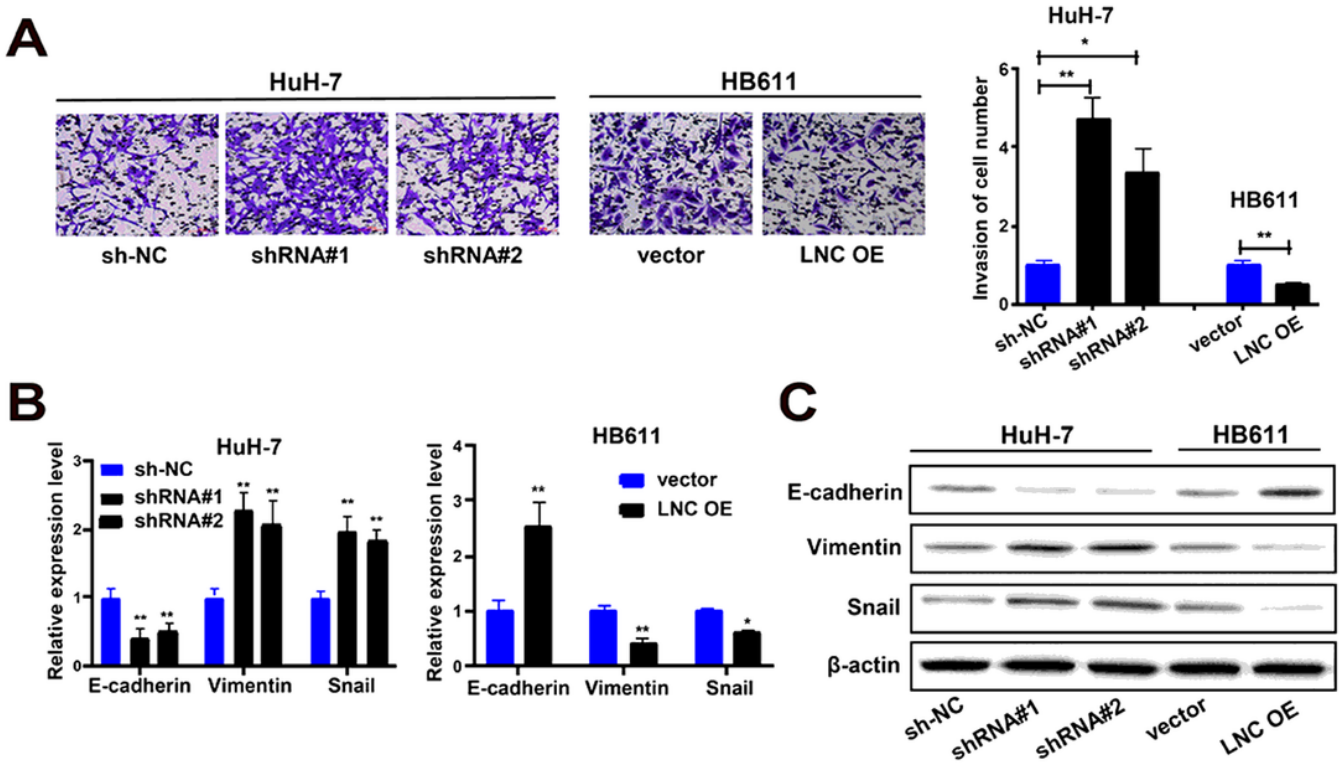

Figure 3

TMEM220-AS1 inhibits cell invasion and EMT of HCC cells (A) Cell invasion was determined using transwell assay. (B, C) The expression of EMT markers were determined using qRT-PCR and western blot assay. Data were presented asrepresent the mean ± SD of 3 independent experiments;*P <0.05, ** P <0.01.

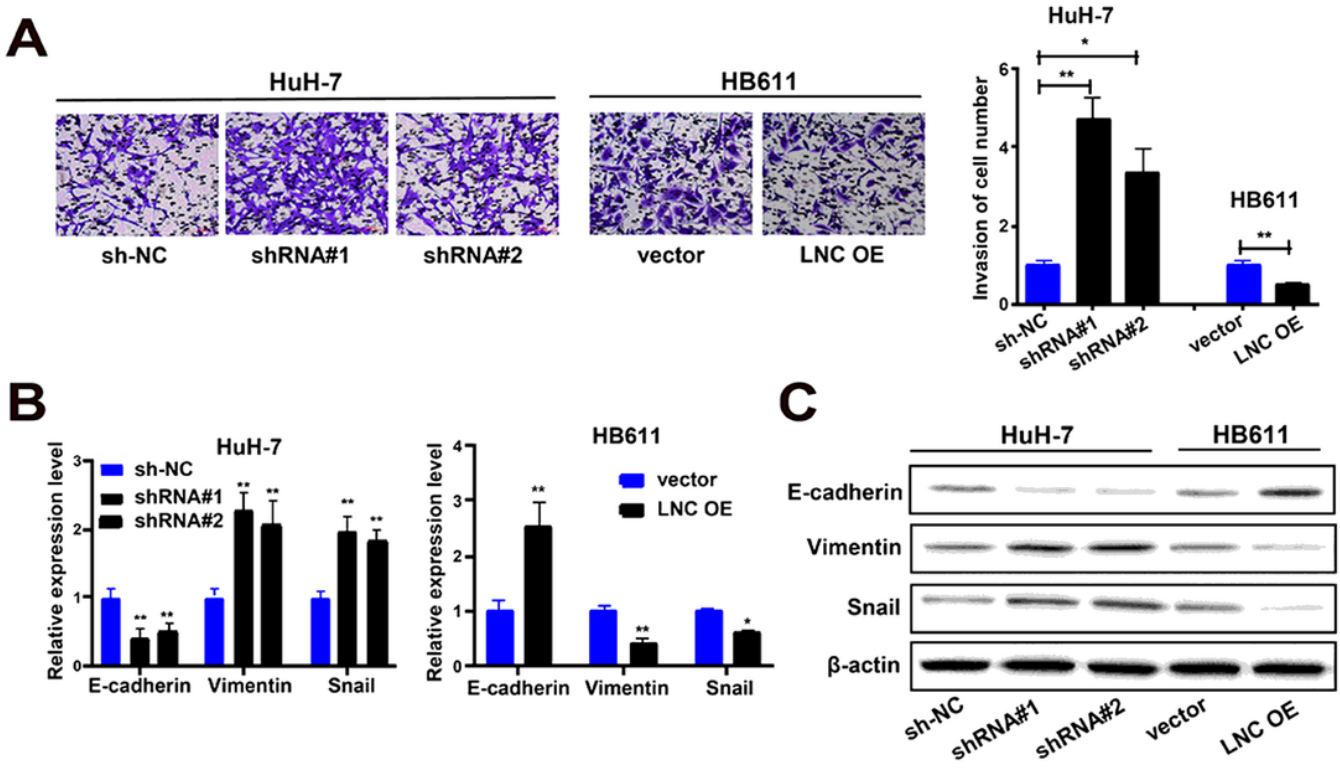

Figure 3

TMEM220-AS1 inhibits cell invasion and EMT of HCC cells (A) Cell invasion was determined using transwell assay. (B, C) The expression of EMT markers were determined using qRT-PCR and western blot assay. Data were presented asrepresent the mean ± SD of 3 independent experiments;*P <0.05, ** P <0.01.

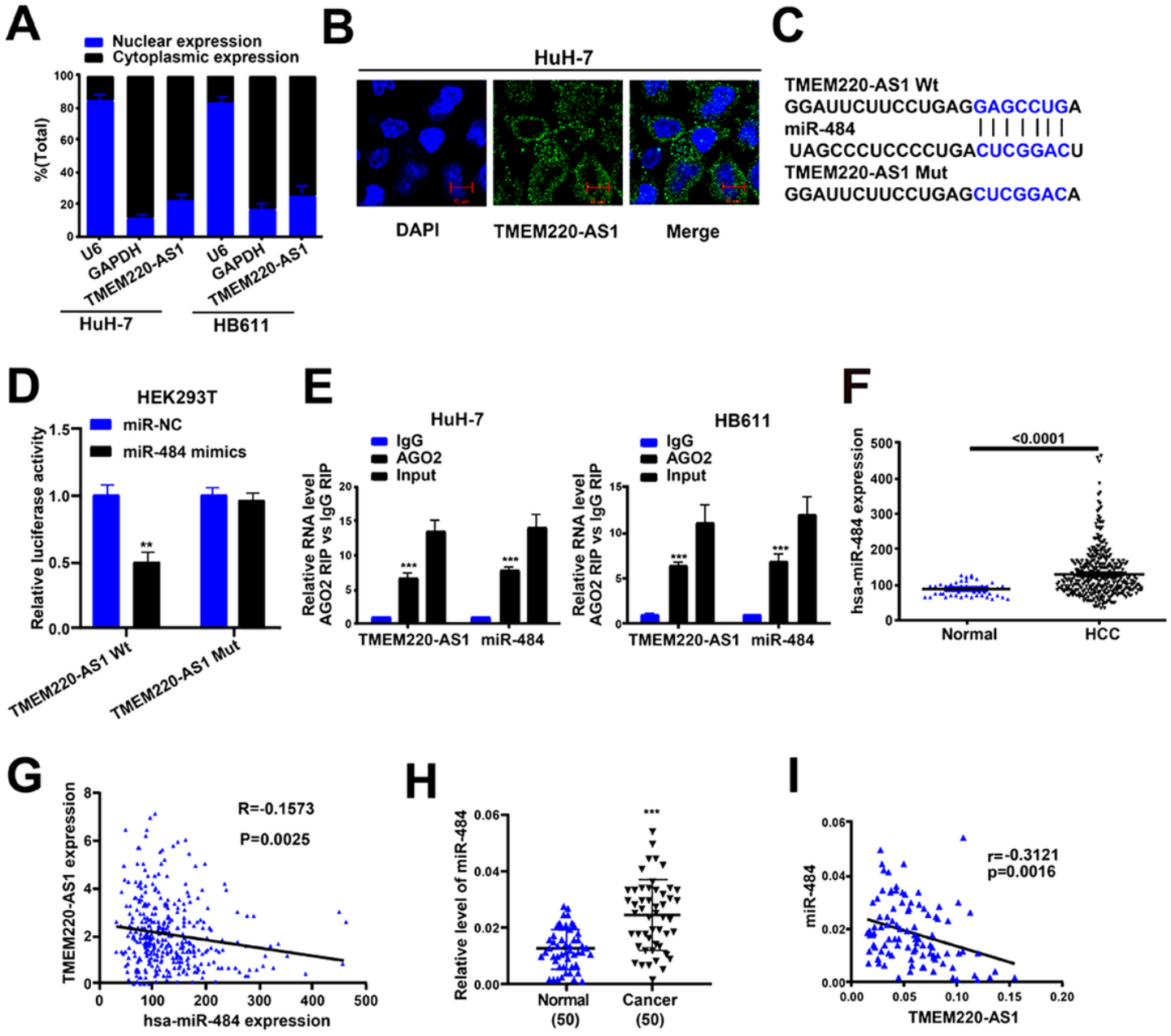

Figure 4

TMEM220-AS1 is targeted by miR-484 (A, B) Localization of TMEM220-AS1 by nucleocytoplasmic separation experiment and RNA-FISH. (C) Putative miR-484 binding sequence and mutation sequence of TMEM220-AS1 mRNA. (D) Dual luciferase reporter assays. (E) RIP assay. (F) miR-484 expression in HCC samples and normal samples, from TCGA database. (G) The correlation analysis between miR-484 expression and TMEM220-AS1 expression in HCC samples and normal samples, from TCGA database. (H) miR-484 expression in HCC tumor tissues,from our samples. (I) The correlation analysis between miR-484 expression and TMEM220-AS1 expression in HCC tumor tissues and adjacent nontumorous tissues, from our samples. Data were presented asrepresent the mean ± SD;** P <0.01, ***P < 0.001.

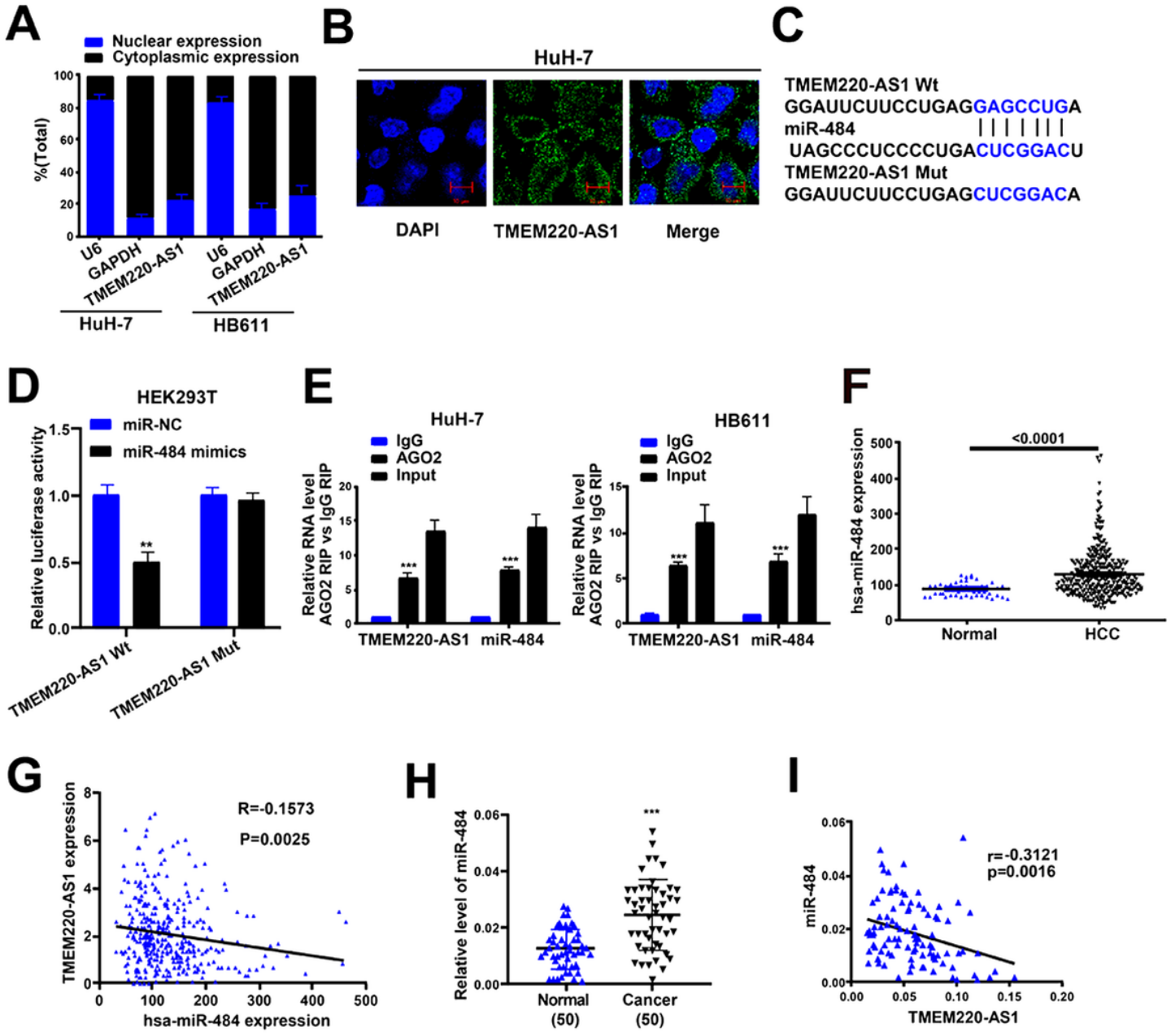

Figure 4

TMEM220-AS1 is targeted by miR-484 (A, B) Localization of TMEM220-AS1 by nucleocytoplasmic separation experiment and RNA-FISH. (C) Putative miR-484 binding sequence and mutation sequence of TMEM220-AS1 mRNA. (D) Dual luciferase reporter assays. (E) RIP assay. (F) miR-484 expression in HCC samples and normal samples, from TCGA database. (G) The correlation analysis between miR-484 expression and TMEM220-AS1 expression in HCC samples and normal samples, from TCGA database. (H) miR-484 expression in HCC tumor tissues,from our samples. (I) The correlation analysis between miR-484 expression and TMEM220-AS1 expression in HCC tumor tissues and adjacent nontumorous tissues, from our samples. Data were presented asrepresent the mean ± SD;** P <0.01, ***P < 0.001.

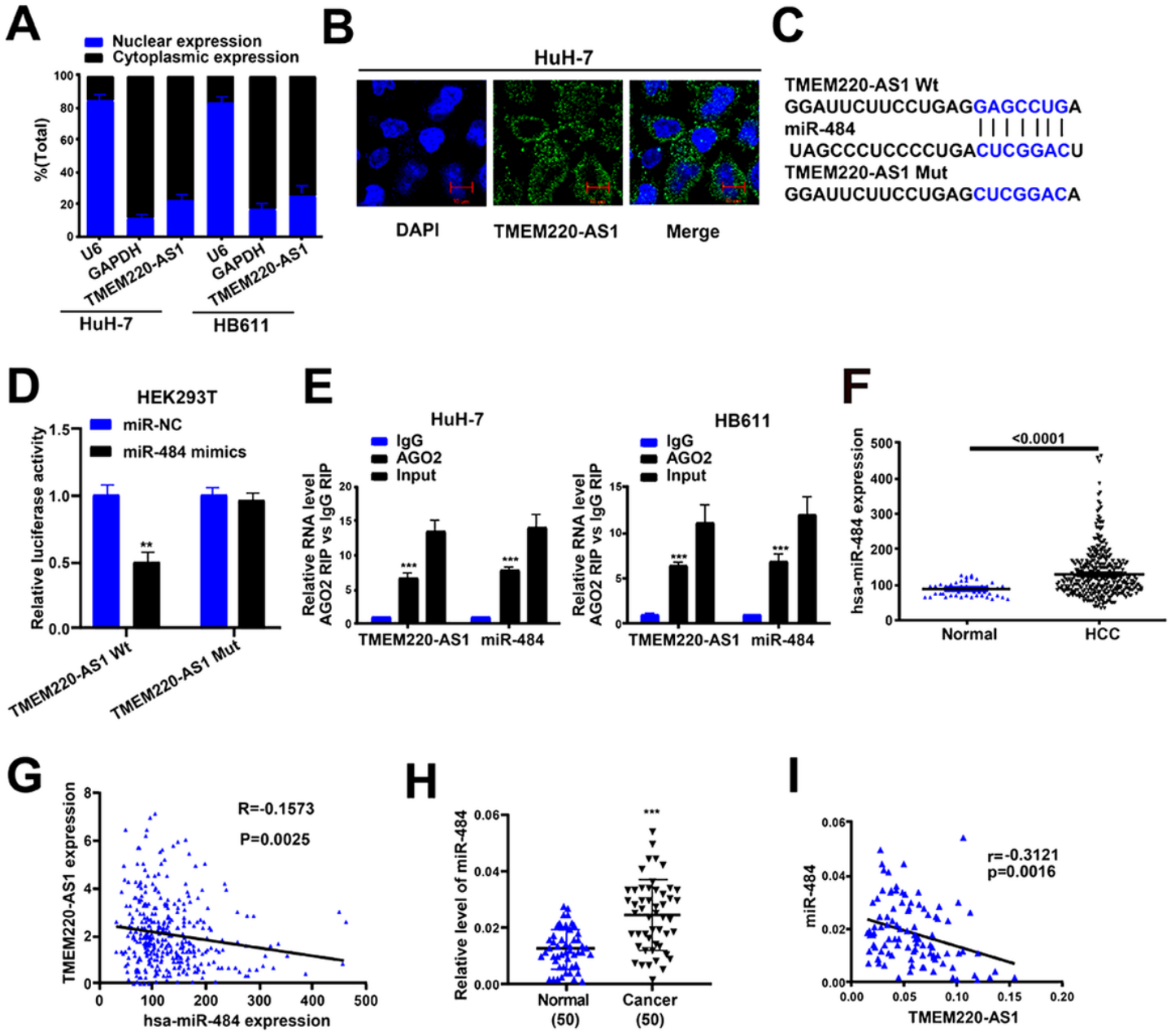

Figure 4

TMEM220-AS1 is targeted by miR-484 (A, B) Localization of TMEM220-AS1 by nucleocytoplasmic separation experiment and RNA-FISH. (C) Putative miR-484 binding sequence and mutation sequence of TMEM220-AS1 mRNA. (D) Dual luciferase reporter assays. (E) RIP assay. (F) miR-484 expression in HCC samples and normal samples, from TCGA database. (G) The correlation analysis between miR-484 expression and TMEM220-AS1 expression in HCC samples and normal samples, from TCGA database. (H) miR-484 expression in HCC tumor tissues,from our samples. (I) The correlation analysis between miR-484 expression and TMEM220-AS1 expression in HCC tumor tissues and adjacent nontumorous tissues, from our samples. Data were presented asrepresent the mean ± SD;** P <0.01, ***P < 0.001.

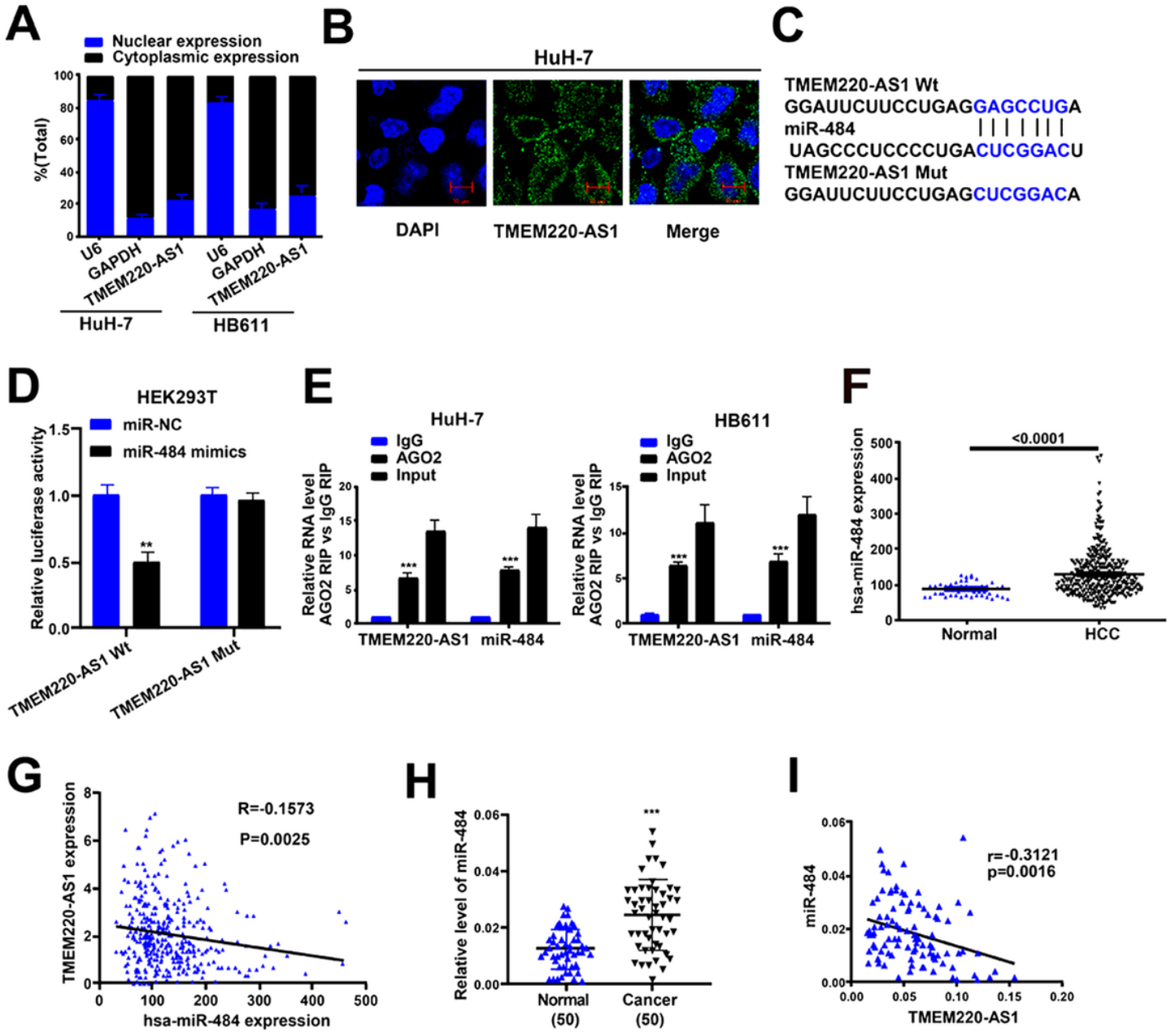

Figure 4

TMEM220-AS1 is targeted by miR-484 (A, B) Localization of TMEM220-AS1 by nucleocytoplasmic separation experiment and RNA-FISH. (C) Putative miR-484 binding sequence and mutation sequence of TMEM220-AS1 mRNA. (D) Dual luciferase reporter assays. (E) RIP assay. (F) miR-484 expression in HCC samples and normal samples, from TCGA database. (G) The correlation analysis between miR-484 expression and TMEM220-AS1 expression in HCC samples and normal samples, from TCGA database. (H) miR-484 expression in HCC tumor tissues,from our samples. (I) The correlation analysis between miR-484 expression and TMEM220-AS1 expression in HCC tumor tissues and adjacent nontumorous tissues, from our samples. Data were presented asrepresent the mean ± SD;** P <0.01, ***P < 0.001.

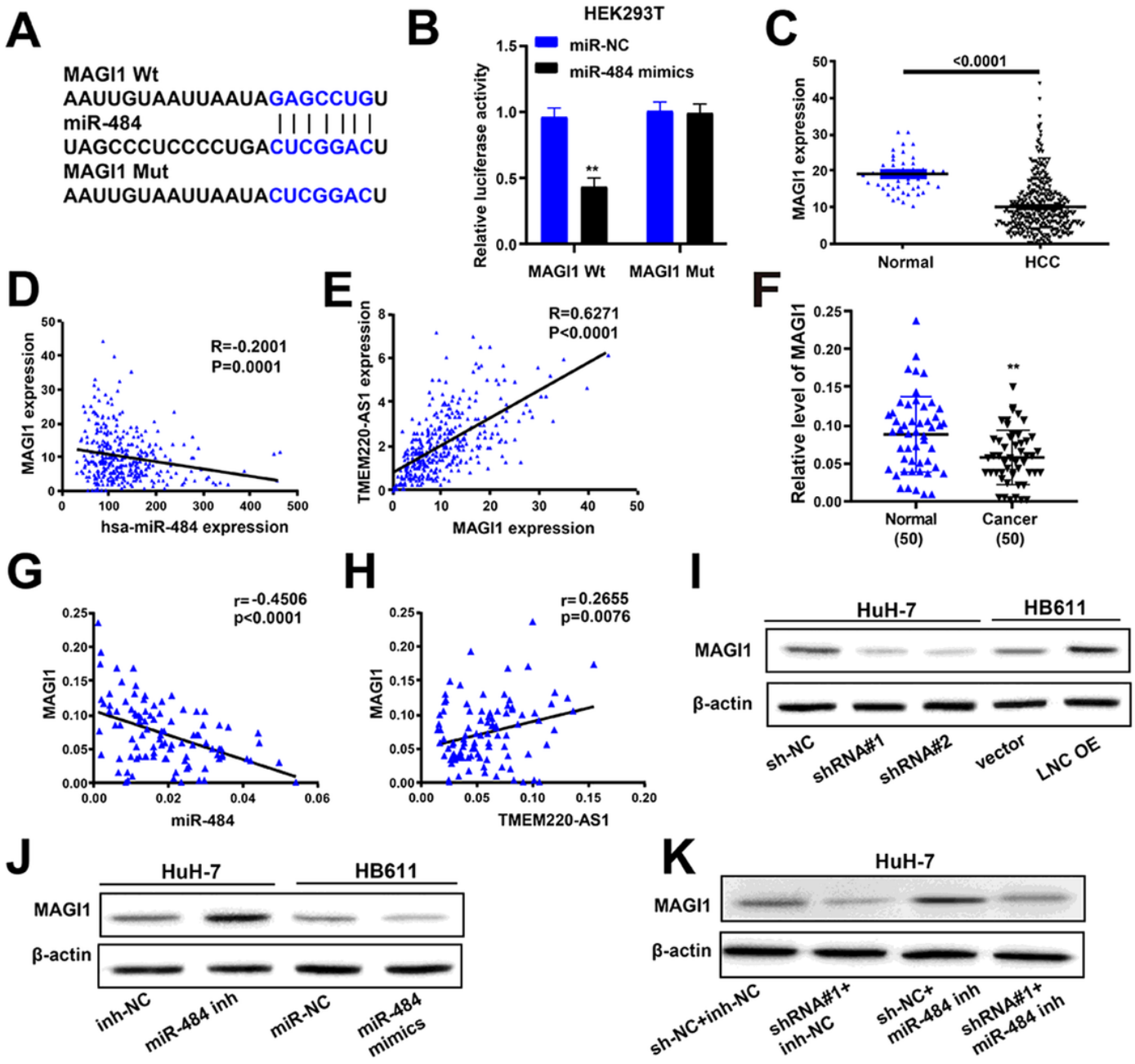

Figure 5

TMEM220-AS1 regulates the miR-484 target gene, MAGI1 (A) Putative miR-484 binding sequence and mutation sequence of MAGI1 mRNA. (B) Dual luciferase reporter assays. (C) MAGI1 gene expression in HCC samples from TCGA database. (D) The correlation analysis between miR-484 expression and MAGI1 expression in HCC samples and normal samples, from TCGA database. (E) The correlation analysis between TMEM220-AS1 expression and MAGI1 expression in HCC samples and normal samples, from TCGA database. (F) MAGI1 gene expression in HCC tissues and paired adjacent normal tissues, from our samples. (G) The correlation analysis between miR-484 expression and MAGI1 expression in HCC tissues and paired adjacent normal tissues, from our samples. (H) The correlation analysis between TMEM220-AS1 expression and MAGI1 expression in HCC tissues and paired adjacent normal tissues, from our

samples. (I-K) The level of MAGI1 was detectedby western blot assay. Data were presented asrepresent the mean ± SD; ** P <0.01, ***P < 0.001.

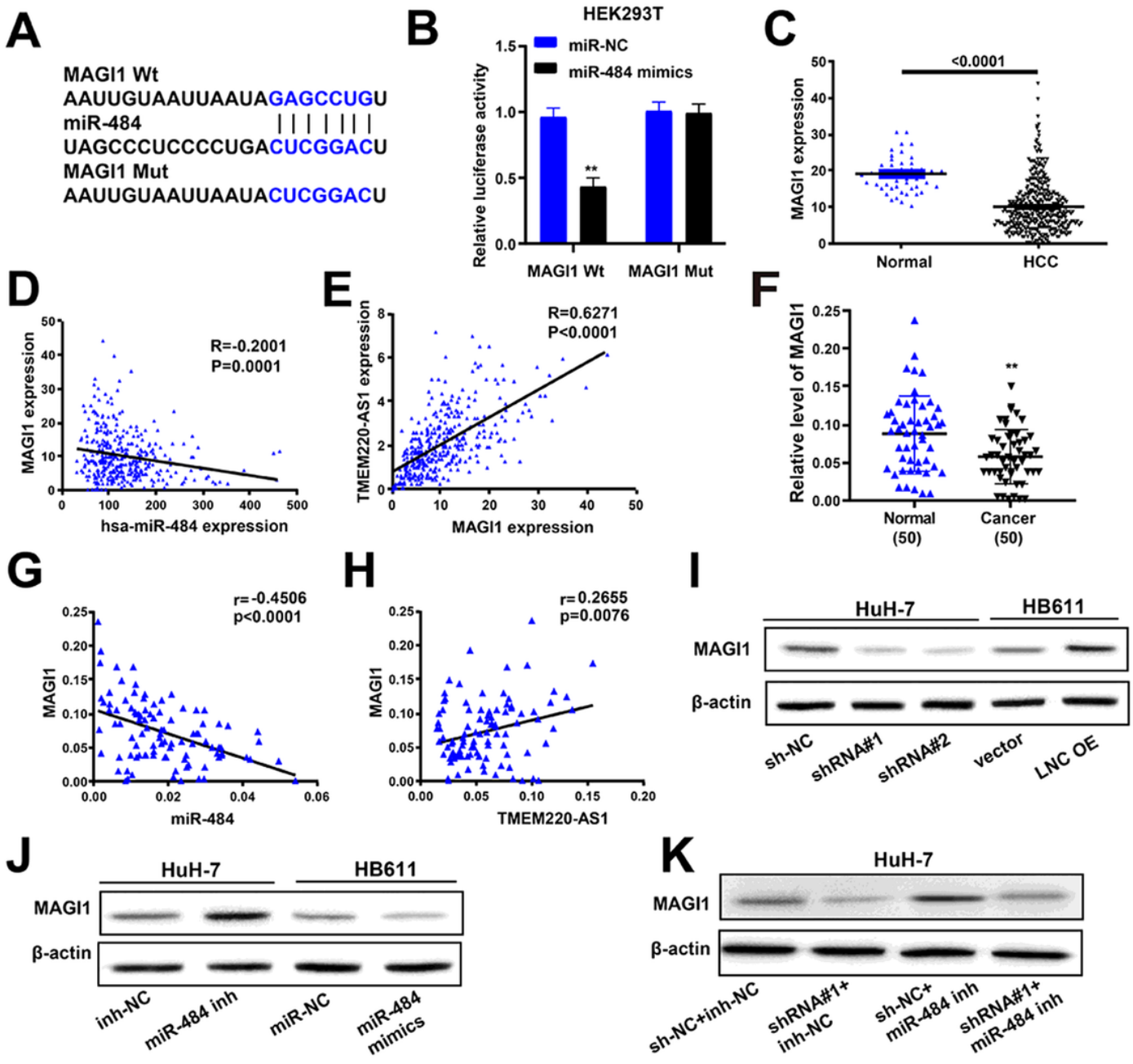

Figure 5

TMEM220-AS1 regulates the miR-484 target gene, MAGI1 (A) Putative miR-484 binding sequence and mutation sequence of MAGI1 mRNA. (B) Dual luciferase reporter assays. (C) MAGI1 gene expression in HCC samples from TCGA database. (D) The correlation analysis between miR-484 expression and MAGI1 expression in HCC samples and normal samples, from TCGA database. (E) The correlation analysis between TMEM220-AS1 expression and MAGI1 expression in HCC samples and normal samples, from TCGA database. (F) MAGI1 gene expression in HCC tissues and paired adjacent normal tissues, from our samples. (G) The correlation analysis between miR-484 expression and MAGI1 expression in HCC tissues

and paired adjacent normal tissues, from our samples. (H) The correlation analysis between TMEM220-AS1 expression and MAGI1 expression in HCC tissues and paired adjacent normal tissues, from our samples. (I-K) The level of MAGI1 was detectedby western blot assay. Data were presented asrepresent the mean ± SD; ** P <0.01, ***P < 0.001.

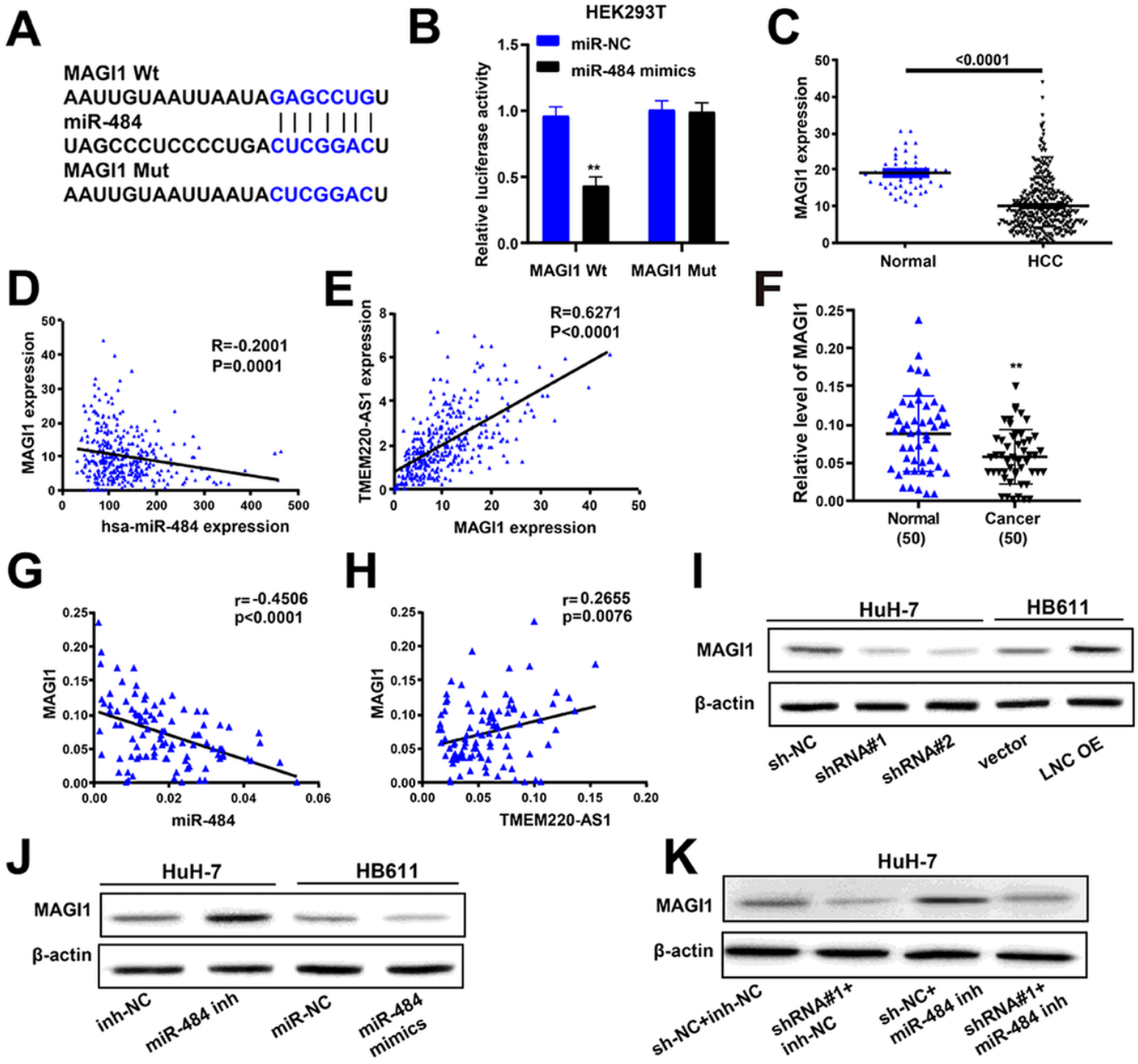

Figure 5

TMEM220-AS1 regulates the miR-484 target gene, MAGI1 (A) Putative miR-484 binding sequence and mutation sequence of MAGI1 mRNA. (B) Dual luciferase reporter assays. (C) MAGI1 gene expression in HCC samples from TCGA database. (D) The correlation analysis between miR-484 expression and MAGI1 expression in HCC samples and normal samples, from TCGA database. (E) The correlation analysis between TMEM220-AS1 expression and MAGI1 expression in HCC samples and normal samples, from

TCGA database. (F) MAGI1 gene expression in HCC tissues and paired adjacent normal tissues, from our samples. (G) The correlation analysis between miR-484 expression and MAGI1 expression in HCC tissues and paired adjacent normal tissues, from our samples. (H) The correlation analysis between TMEM220-AS1 expression and MAGI1 expression in HCC tissues and paired adjacent normal tissues, from our samples. (I-K) The level of MAGI1 was detectedby western blot assay. Data were presented asrepresent the mean ± SD; ** P <0.01, ***P < 0.001.

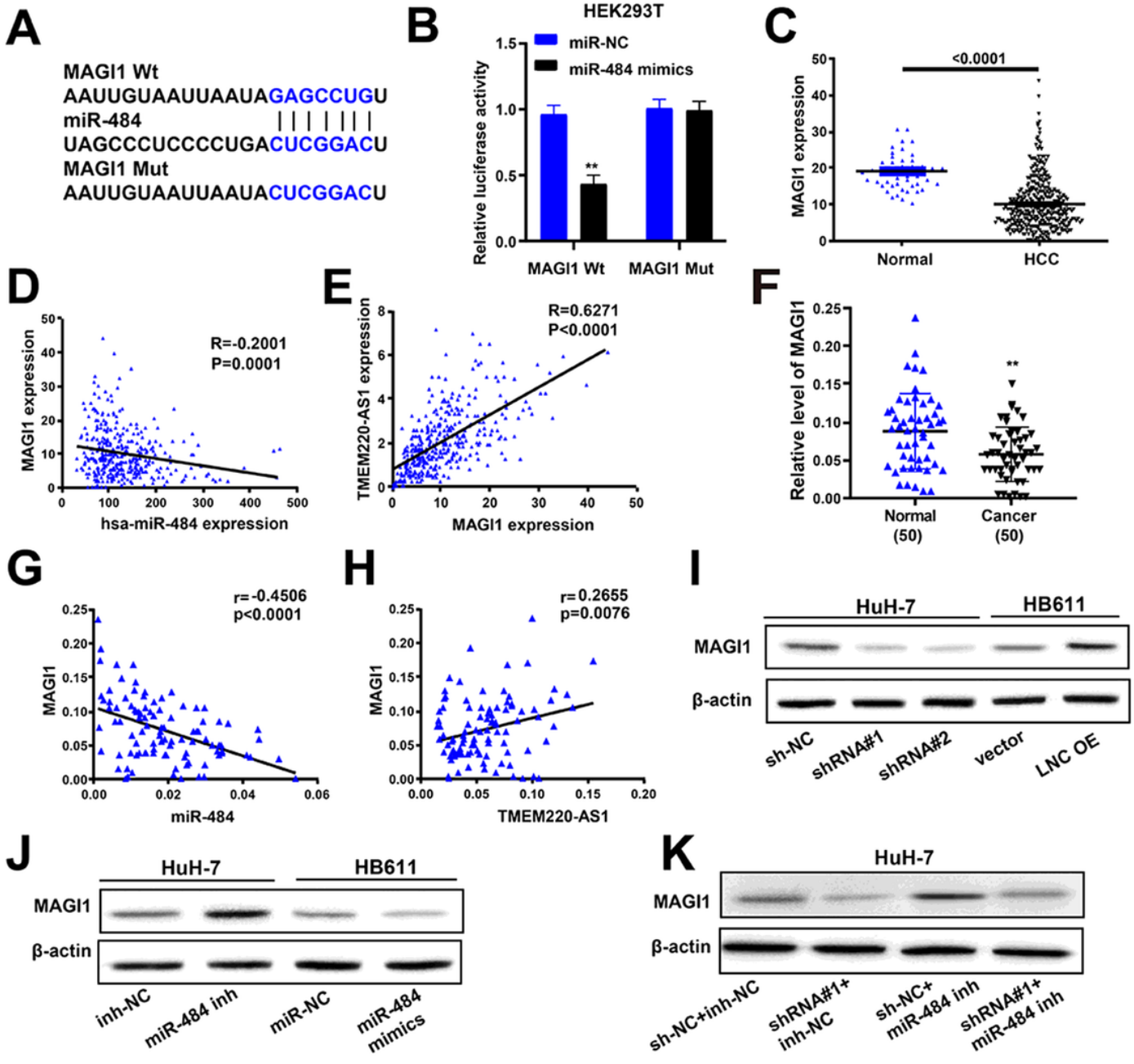

Figure 5

TMEM220-AS1 regulates the miR-484 target gene, MAGI1 (A) Putative miR-484 binding sequence and mutation sequence of MAGI1 mRNA. (B) Dual luciferase reporter assays. (C) MAGI1 gene expression in HCC samples from TCGA database. (D) The correlation analysis between miR-484 expression and MAGI1

expression in HCC samples and normal samples, from TCGA database. (E) The correlation analysis between TMEM220-AS1 expression and MAGI1 expression in HCC samples and normal samples, from TCGA database. (F) MAGI1 gene expression in HCC tissues and paired adjacent normal tissues, from our samples. (G) The correlation analysis between miR-484 expression and MAGI1 expression in HCC tissues and paired adjacent normal tissues, from our samples. (H) The correlation analysis between TMEM220-AS1 expression and MAGI1 expression in HCC tissues and paired adjacent normal tissues, from our samples. (I-K) The level of MAGI1 was detectedby western blot assay. Data were presented asrepresent the mean ± SD; ** P <0.01, ***P < 0.001.

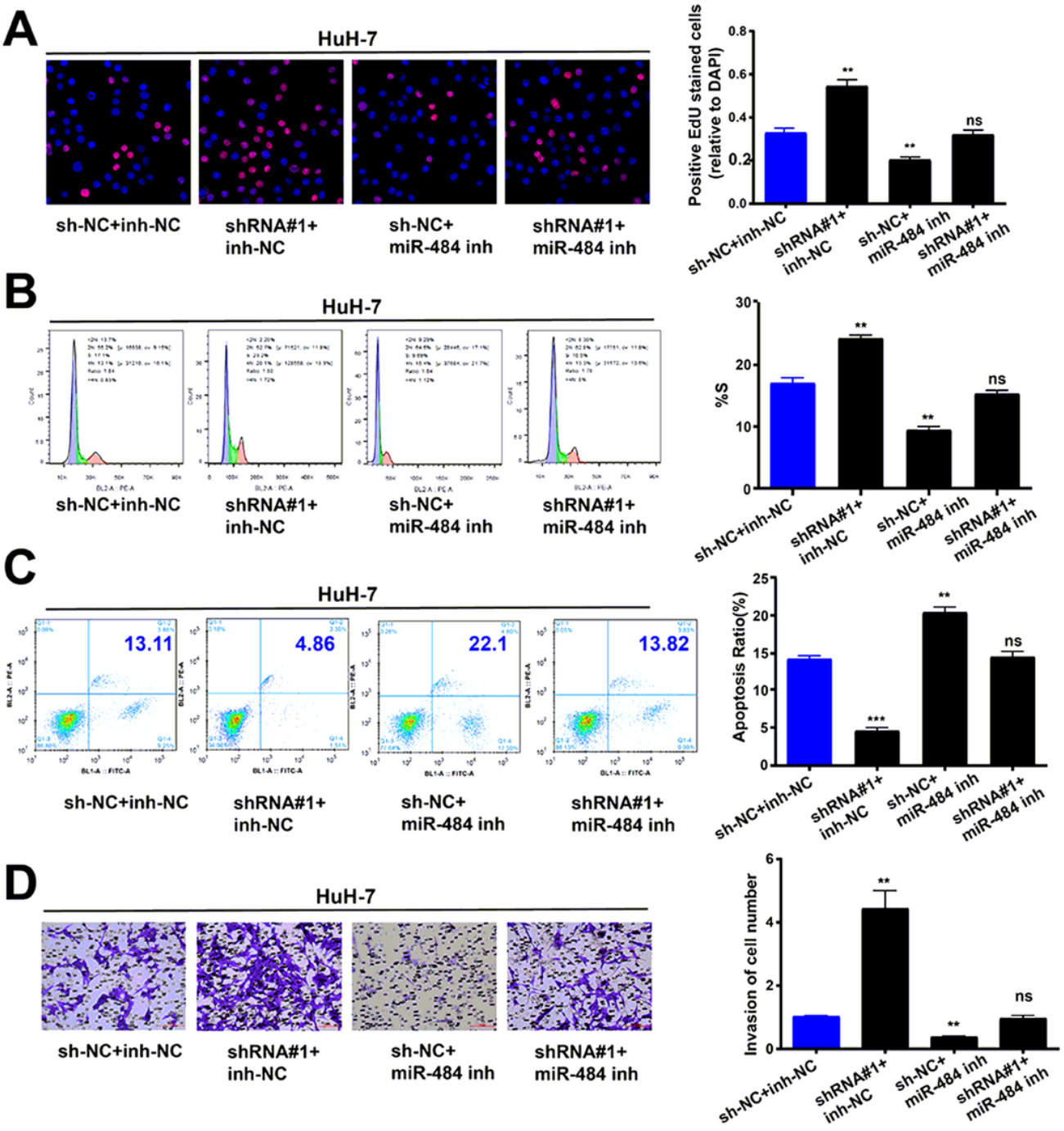

Figure 6

TMEM220-AS1/miR-484 axis regulates behaviors of HCC cells (A) Cell proliferation. (B) Cell cycle. (C) Cell apoptosis. (D) Cell invasion. Data were presented asrepresent the mean ± SD of 3 independent experiments;** P <0.01, ***P < 0.001, ns: no significance.

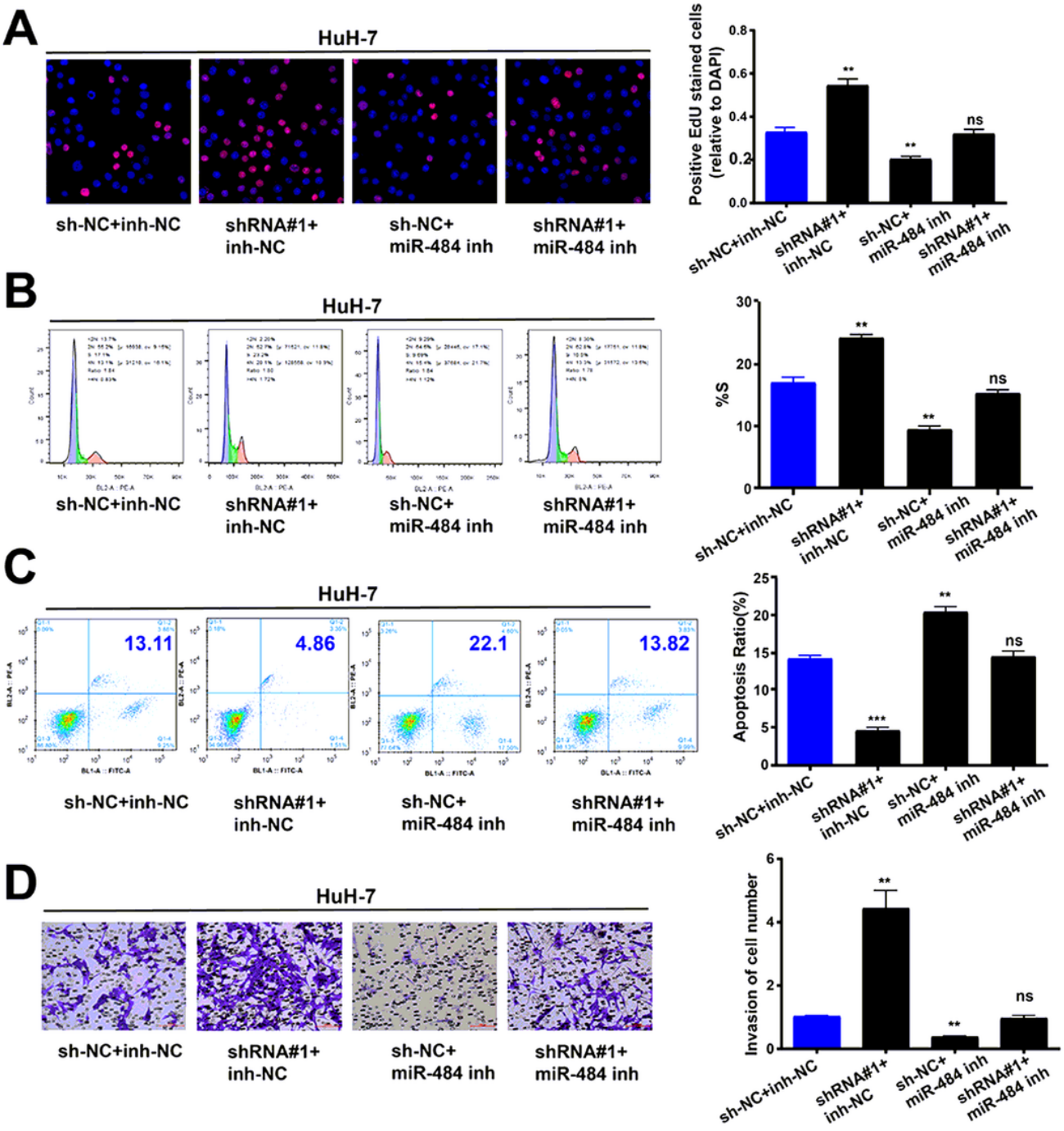

Figure 6

TMEM220-AS1/miR-484 axis regulates behaviors of HCC cells (A) Cell proliferation. (B) Cell cycle. (C) Cell apoptosis. (D) Cell invasion. Data were presented asrepresent the mean ± SD of 3 independent experiments;** P <0.01, ***P < 0.001, ns: no significance.

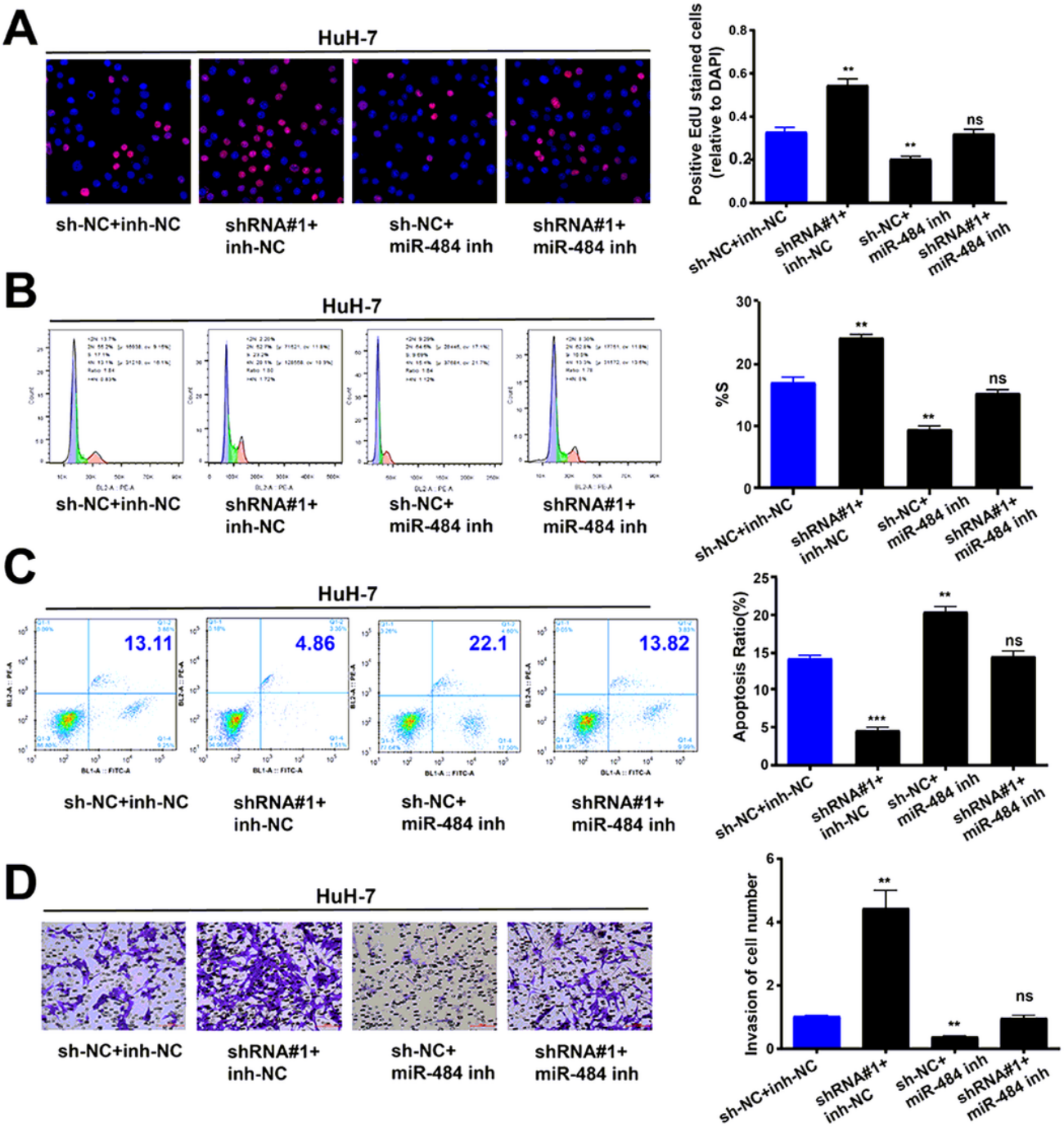

Figure 6

TMEM220-AS1/miR-484 axis regulates behaviors of HCC cells (A) Cell proliferation. (B) Cell cycle. (C) Cell apoptosis. (D) Cell invasion. Data were presented asrepresent the mean ± SD of 3 independent experiments;** P <0.01, ***P < 0.001, ns: no significance.

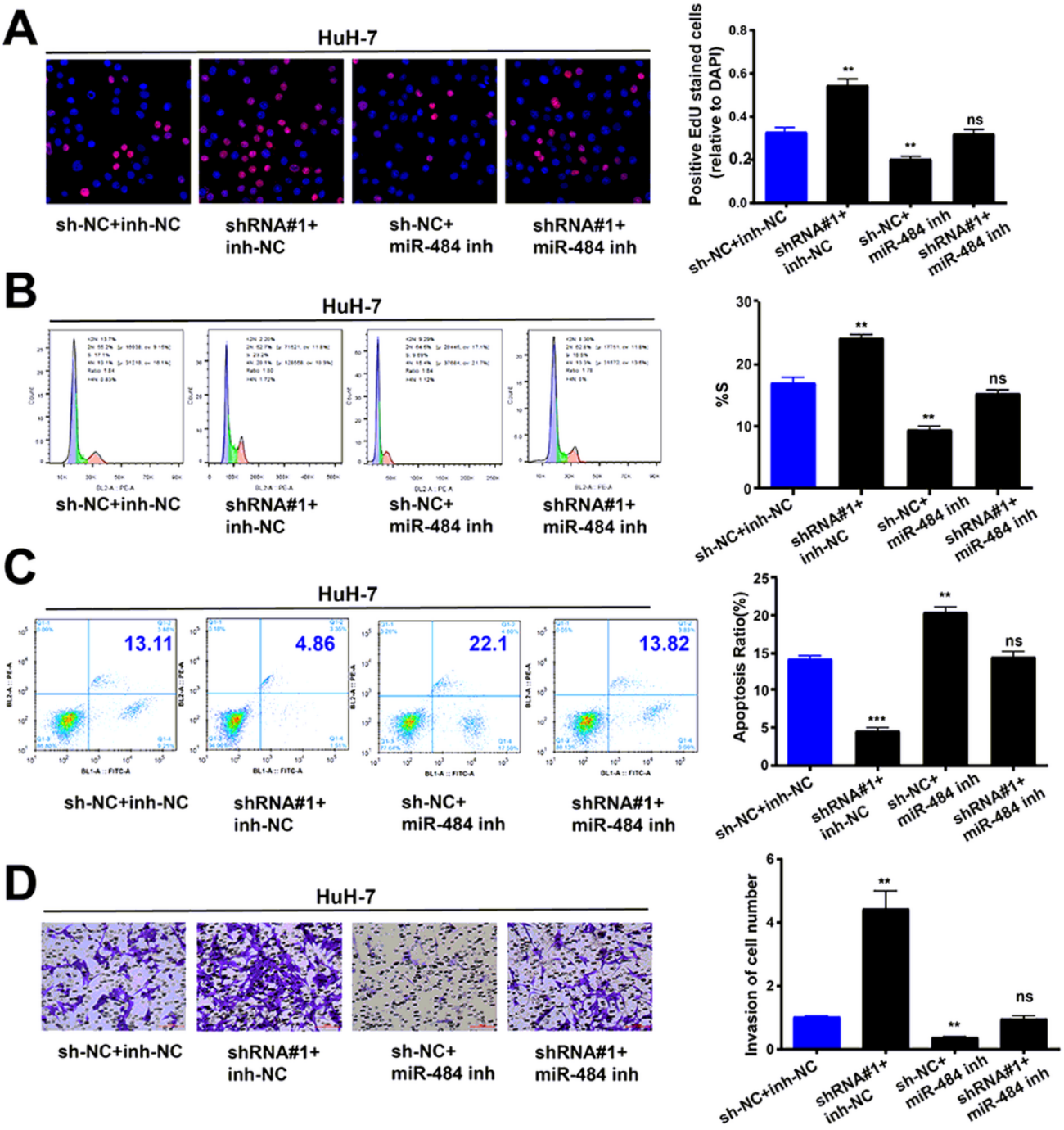

Figure 6

TMEM220-AS1/miR-484 axis regulates behaviors of HCC cells (A) Cell proliferation. (B) Cell cycle. (C) Cell apoptosis. (D) Cell invasion. Data were presented asrepresent the mean ± SD of 3 independent experiments;** P <0.01, ***P < 0.001, ns: no significance.

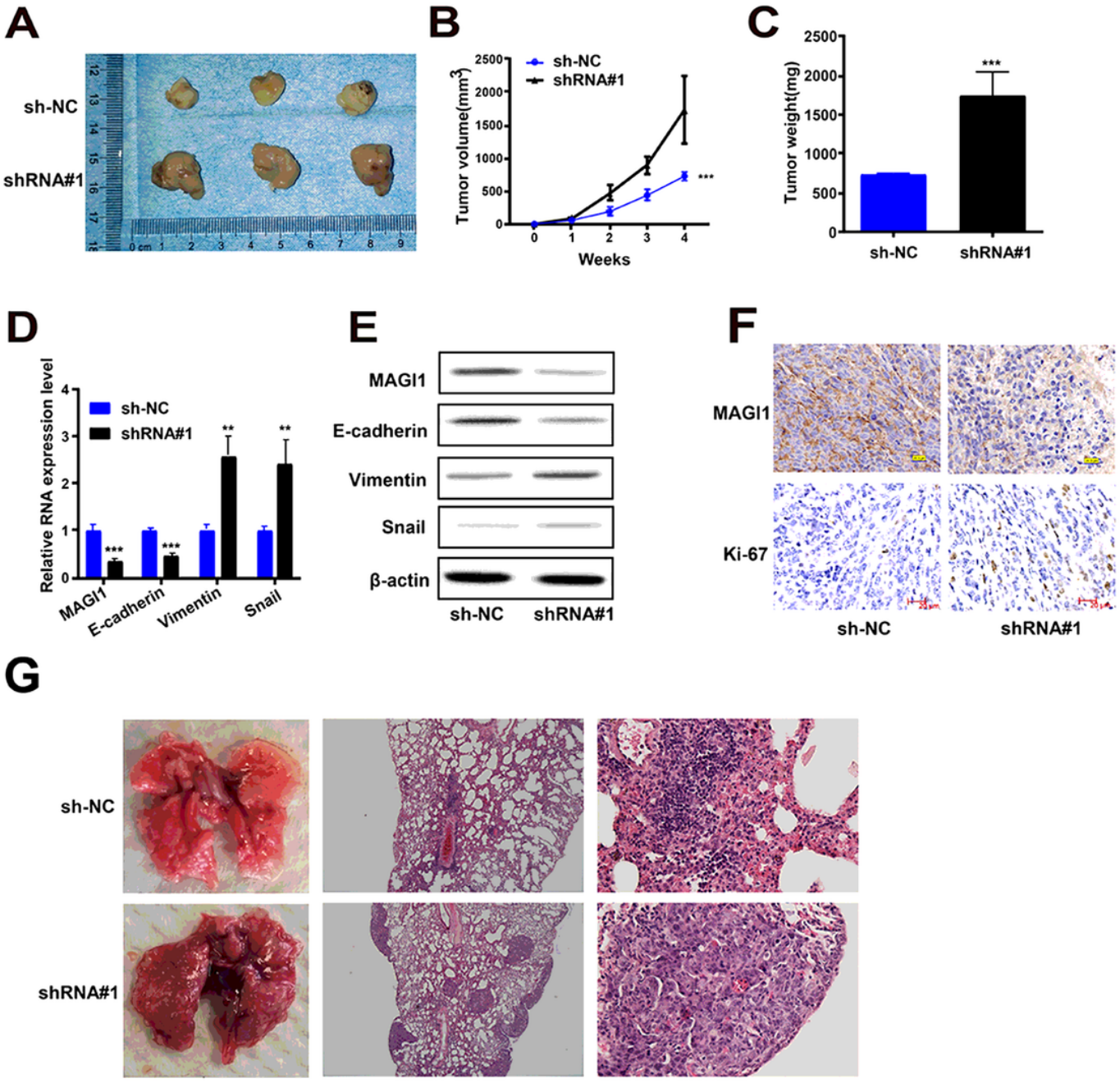

Figure 7

TMEM220-AS1knockdown promotes growthand metastasis of HCC cells in vivo (A) Representative images of xenografts. (B) Tumor volume and (C) weight data of indicated orthotopic xenografts. (D, E) mRNA and protein expression levels of MAGI1 and EMT-related markers after TMEM220-AS1 knockdown. (F) The expression level of MEGI1 and Ki-67 determined using immunohistochemistry. (G) Representative images of lung metastases of indicated orthotopic xenografts. Data were presented asrepresent the mean ± SD;** P <0.01, ***P < 0.001.

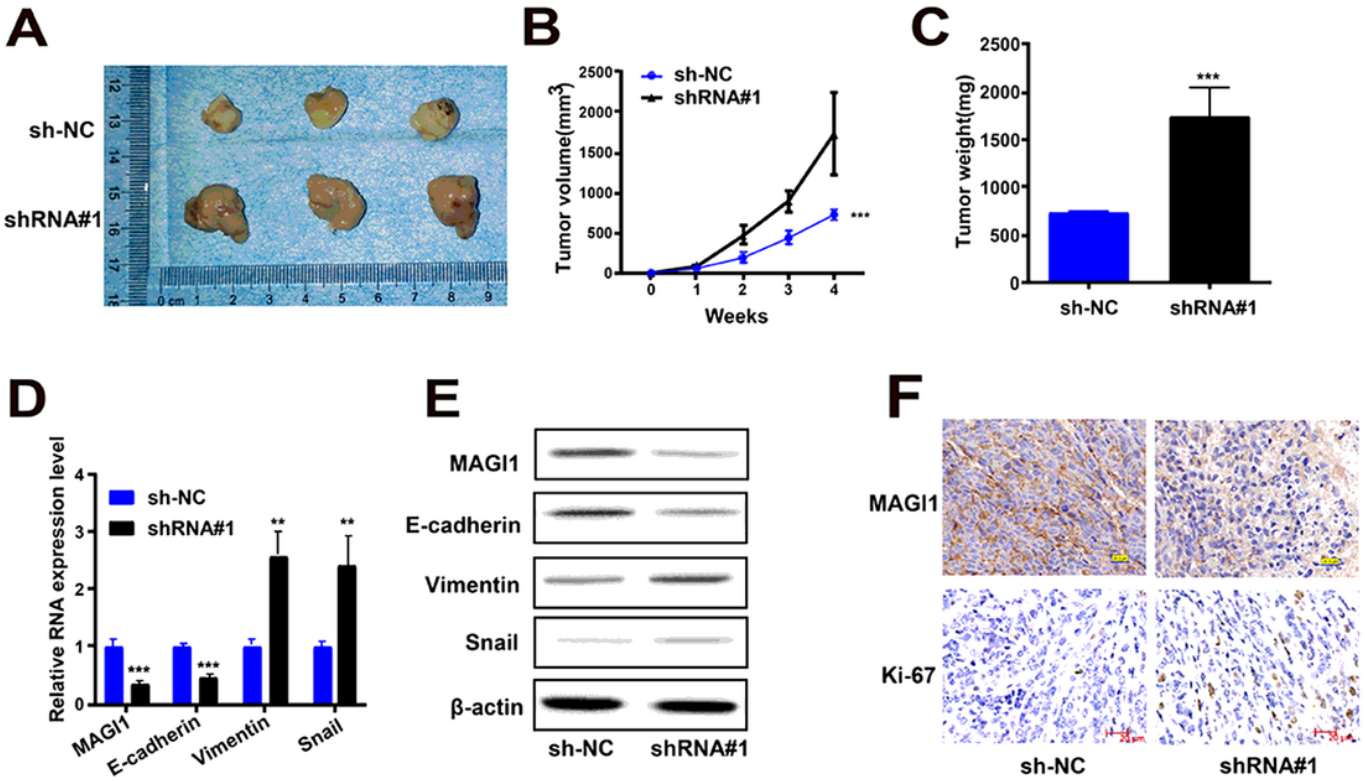

Figure 7

TMEM220-AS1knockdown promotes growthand metastasis of HCC cells in vivo (A) Representative images of xenografts. (B) Tumor volume and (C) weight data of indicated orthotopic xenografts. (D, E) mRNA and protein expression levels of MAGI1 and EMT-related markers after TMEM220-AS1 knockdown. (F) The expression level of MEGI1 and Ki-67 determined using immunohistochemistry. (G) Representative images of lung metastases of indicated orthotopic xenografts. Data were presented asrepresent the mean ± SD;** P <0.01, ***P < 0.001.

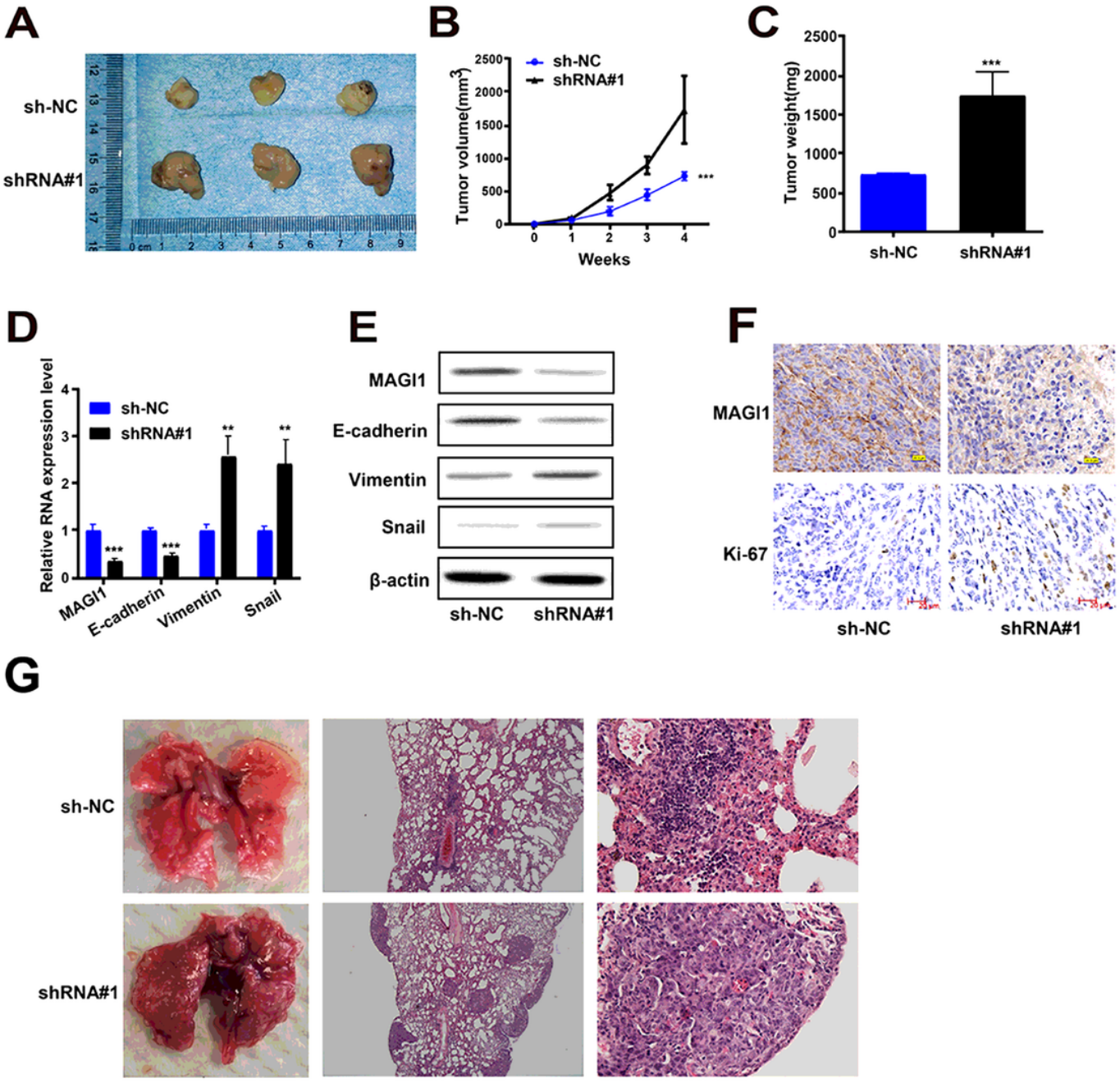

Figure 7

TMEM220-AS1knockdown promotes growthand metastasis of HCC cells in vivo (A) Representative images of xenografts. (B) Tumor volume and (C) weight data of indicated orthotopic xenografts. (D, E) mRNA and protein expression levels of MAGI1 and EMT-related markers after TMEM220-AS1 knockdown. (F) The expression level of MEGI1 and Ki-67 determined using immunohistochemistry. (G) Representative images of lung metastases of indicated orthotopic xenografts. Data were presented asrepresent the mean ± SD;** P <0.01, ***P < 0.001.

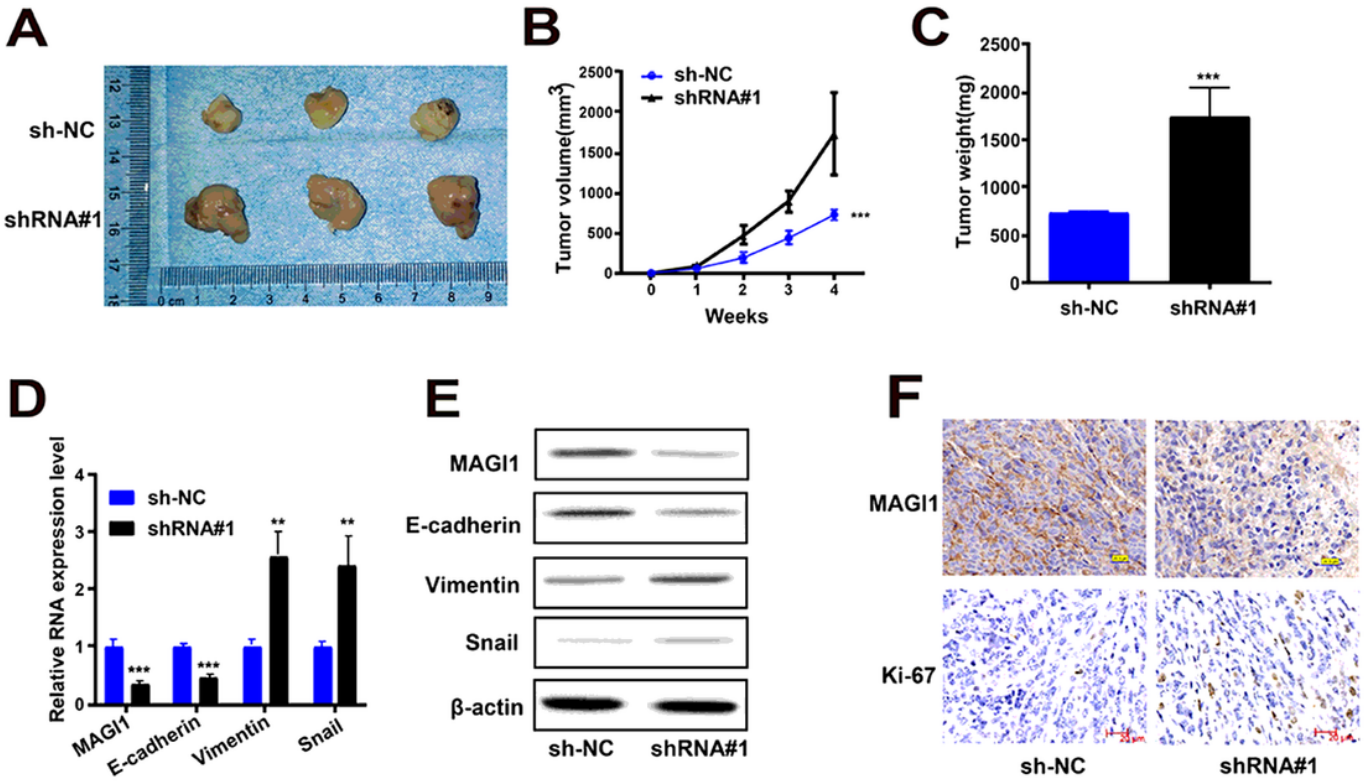

Figure 7

TMEM220-AS1knockdown promotes growthand metastasis of HCC cells in vivo (A) Representative images of xenografts. (B) Tumor volume and (C) weight data of indicated orthotopic xenografts. (D, E) mRNA and protein expression levels of MAGI1 and EMT-related markers after TMEM220-AS1 knockdown. (F) The expression level of MEGI1 and Ki-67 determined using immunohistochemistry. (G) Representative images of lung metastases of indicated orthotopic xenografts. Data were presented asrepresent the mean ± SD;** P <0.01, ***P < 0.001.

Supplementary Files

This is a list of supplementary files associated with this preprint. Click to download.

- SupplementaryFigure1legend.docx
- SupplementaryFigure1legend.docx
- SupplementaryFigure1legend.docx
- SupplementaryFigure1legend.docx
- SupplementrayFigure1.tif
- SupplementrayFigure1.tif
- SupplementrayFigure1.tif
- SupplementrayFigure1.tif
- SupplementaryMethods.docx
- SupplementaryMethods.docx
- SupplementaryMethods.docx
- SupplementaryMethods.docx
- SupplementaryTable1.docx
- SupplementaryTable1.docx
- SupplementaryTable1.docx
- SupplementaryTable1.docx